

National Astronomy and Ionosphere Center

## **Arecibo Observatory**

### **Focal Array Memo Series**

# **Multi Beam Array System Feed Selection**

By: Germán Cortés-Medellín

**CORNELL**  
University

July/29/2001  
Rev. 02



National Science  
Foundation

**INDEX**

1.	Introduction.....	4
2.	Antenna Analysis Methodology .....	5
2.1	Feed Horn Simulation .....	5
2.1.1	Frequency Band .....	5
2.1.2	Polarization .....	5
2.1.3	Radiation Patterns .....	5
2.1.4	Edge Taper Angle .....	5
2.1.5	Input Circular Waveguide.....	5
2.2	Antenna Gain and G/T Analysis .....	5
3.	Feed Horn Characteristics.....	6
3.1	First Coaxial and TE <sub>11</sub> Mode Horn Set: 15.3 cm Aperture.....	6
3.1.1	TE <sub>11</sub> Mode Horn Geometry.....	6
3.1.2	Lovell's Coaxial feed Horn Geometry.....	6
3.2	Second Coaxial and TE <sub>11</sub> Mode Horn Set: 19.0 cm Aperture .....	7
3.2.1	TE <sub>11</sub> Mode Feed Horn Geometry.....	7
3.2.2	Coaxial Feed Horn Geometry .....	7
3.3	Third Coaxial and TE <sub>11</sub> Mode Horn Set.....	8
3.3.1	Bird's Coaxial Feed Horn Geometry (19.6 cm Aperture Diameter) .....	8
3.3.2	Parkes TE <sub>11</sub> Mode Feed Horn (24.0 cm Aperture Diameter) .....	8
3.3.3	TE <sub>11</sub> Mode Feed Horn (26.0 cm Aperture Diameter).....	9
4.	Feed Far Field Radiation Patterns.....	10
4.1	Radiation Patterns: 15.3 cm Aperture Coaxial and TE <sub>11</sub> Mode Horn Set.....	10
4.1.1	TE <sub>11</sub> Mode Horn Far Field Patterns .....	10
4.1.2	Lovell's Coaxial Horn Far Field Patterns .....	10
4.2	Radiation Patterns: 19.0 cm Aperture Coaxial and TE <sub>11</sub> Mode Horn Set.....	17
4.2.1	TE <sub>11</sub> Mode Horn Far Field Patterns .....	17
4.2.2	Coaxial Feed Horn Far Field Patterns.....	17
4.3	Radiation Patterns: Coaxial and TE <sub>11</sub> Mode Horn Set (Various Apertures)....	24
4.3.1	Bird's 19.6 cm aperture Coaxial Feed Horn Patterns .....	24
4.3.2	Parkes 24.0 cm aperture TE <sub>11</sub> Mode Feed Horn Patterns .....	24
4.3.3	TE <sub>11</sub> Mode 26.0 cm aperture Feed Horn Patterns .....	24
4.4	Discussion.....	34
4.5	What About Input Matching? .....	34
5.	Multibeam Array Layout and Field of View .....	36
5.1	Arecibo Gregorian System Optics .....	36
5.2	Feed Array Geometry .....	36
5.3	Field of View and Scanning Losses.....	37
6.	Overall Array Performance.....	39
6.1	Central Pixel Antenna Effective Aperture/Gain vs. Frequency.....	39
6.2	Antenna Effective Aperture for each Pixel vs. Frequency .....	40
6.3	Discussion.....	44
7.	Feed array and Antenna G/T Performance .....	45
7.1	Antenna Noise Analysis Assumptions.....	45
7.2	Antenna G/T for each Pixel vs. Frequency.....	46

7.3 Discussion..... 50  
8. Summary and Conclusions ..... 51  
8.1 Conclusions..... 51

# 1. Introduction

This document presents a comprehensive study of seven feed types analyzed for the Arecibo Multi-Beam Array System.

The purpose of this study was to obtain sufficient information regarding the feeds performance, not only as a single device, but, particularly, embedded in the Gregorian system optics including noise temperature analysis in order to provide a clear basis for a selection.

The seven feeds studied are divided in three sets of TE<sub>11</sub> mode and coaxial horns.

Feed Horn Type		Aperture Diameter
1	TE <sub>11</sub> Mode	15.3 cm
2	Lowell's Coaxial	15.3 cm
3	TE <sub>11</sub> Mode	19.0 cm
4	Coaxial	19.0 cm
5	Bird's Coaxial	19.6 cm
6	Parkes TE <sub>11</sub> Mode	24.0 cm
7	TE <sub>11</sub> Mode	26.0 cm

The first two sets (TE<sub>11</sub> mode and coaxial horns) are part of a comparative study between TE<sub>11</sub> mode and coaxial horns for the Arecibo Gregorian multi beam system and for which we have the geometry readily available. The TE<sub>11</sub> mode feed horn with 15.3 cm in diameter is simply a circular waveguide. The coaxial horn of 15.3 cm in diameter is used in the Lovell's radio telescope<sup>1</sup>.

The second set of TE<sub>11</sub> mode and coaxial horns, with an aperture of 19.0 cm, are based on a preliminary design.

The third set of horns corresponds to more particular horns, which are being considered as candidates for the multi-beam system. Among these is the 24.0 cm TE<sub>11</sub> mode horn used for Parkes radio telescope array<sup>2</sup>. Another candidate for the array is a coaxial horn of 19.6 cm aperture designed by Dr. Trevor Bird (CSIRO). Also in this third set of horns we have included a 26.0 cm aperture TE<sub>11</sub> mode horn, optimized for matching, with a return loss  $\geq 25$ . dB. This horn size produces the optimum performance for a TE<sub>11</sub> mode horn array embedded in the Arecibo Gregorian Optics.

<sup>1</sup> T.S. Bird, "Coaxial Feed Array for a Short Focal-Length Reflector". IEEE Ant and P Symposium, 1997

<sup>2</sup> D.B. Hayman & T.S. Bird, "Parkes Multibeam Feed-Horn Measurements". CSIRO Division of Radiophysics, RPP 3803, Australia, Nov. 1995

## 2. Antenna Analysis Methodology

### 2.1 Feed Horn Simulation

The feed simulation proceeded in the following manner: First, a commercial CAD program was used to create a drawing with the detail dimensions of the horn geometry. Second, a full wave finite-element electromagnetic simulator, known as Ansoft's, High Frequency Structure Simulator (HFSS<sup>®</sup>) was used to obtain the fields inside of the feed horn as well as the far field radiation patterns.

Initial specifications of the horns included the following frequency band and polarization:

#### 2.1.1 Frequency Band

For each horn we analyzed three frequency points in the L-Band:

- 1.225 GHz
- 1.375 GHz
- 1.525 GHz

#### 2.1.2 Polarization

The horns were linearly polarized (VERT or HORZ).

#### 2.1.3 Radiation Patterns

For each feed, and except for the 19.6 cm coaxial horn<sup>3</sup>, Ansoft's, HFSS<sup>®</sup> was used to obtain three frequency sets of far field radiation patterns ( $\theta \leq 180$  deg, two cuts); with both ( $E_\theta$ ,  $E_\phi$ ) magnitude and phase for each cut.

#### 2.1.4 Edge Taper Angle

The tertiary reflector edge of the Arecibo Gregorian System is at an angle of 60° with respect the optical axis of the feeds.

#### 2.1.5 Input Circular Waveguide

In all cases, and following Parkes' array design for consistency, the feed input circular waveguide diameter<sup>4</sup> is 15.3 cm, unless otherwise stated.

### 2.2 Antenna Gain and G/T Analysis

Once the feed patterns were obtained, we perform a complete antenna gain analysis of the Arecibo radio telescope optics for each set of feed's radiation patterns, by a combination of spherical wave expansion of the feed radiation patterns, kinematics and electrostatics ray tracing, and aperture field integration. Finally, we performed a noise analysis as seen by the feed to obtain the overall G/T, using all previous techniques in conjunction with a detailed Gregorian noise mapping.

---

<sup>3</sup> The feed patterns for the 19.6 cm coaxial horn were provided directly by Dr. Bird.

<sup>4</sup> However, it must be noted that for a circular waveguide of 15.3 cm in diameter, the  $TM_{01}$  mode cutoff frequency is 1.500 GHz. Therefore, for the final design, it is recommended that a slightly smaller input waveguide diameter be used, i.e., an input diameter of 15.0 cm will put the cutoff frequency of this spurious mode at 1.530 GHz, and away of the bandwidth of interest of 1.225 to 1.525 GHz

### 3. Feed Horn Characteristics

#### 3.1 First Coaxial and TE<sub>11</sub> Mode Horn Set: 15.3 cm Aperture

##### 3.1.1 TE<sub>11</sub> Mode Horn Geometry

Figure 3.1 shows the geometry of this feed, which is a simple Circular Waveguide (CWG) of 15.3 cm in diameter with a length of 50.0 cm.

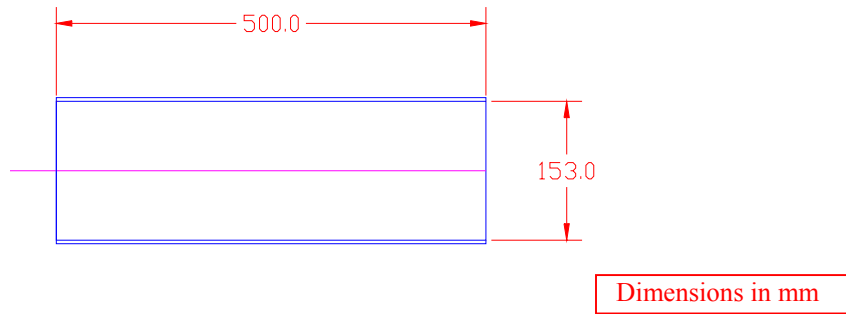


**Figure 3.1 TE<sub>11</sub> mode feed Geometry, (15.3 cm aperture diameter)**

##### 3.1.2 Lovell’s Coaxial feed Horn Geometry

Figure 3.2 shows the feed geometry for this 15.3 cm aperture coaxial design<sup>5</sup>, with an aperture diameter of 2a=15.3 cm, and 2b=8.0 cm, used in the 4 element Multibeam feed for the Lovell radio telescope at Jodrell Bank, UK.

In our simulation we didn’t include three high-density, low-loss polystyrene spacers that are used in the actual horn to hold the coaxial center conductor in place the.

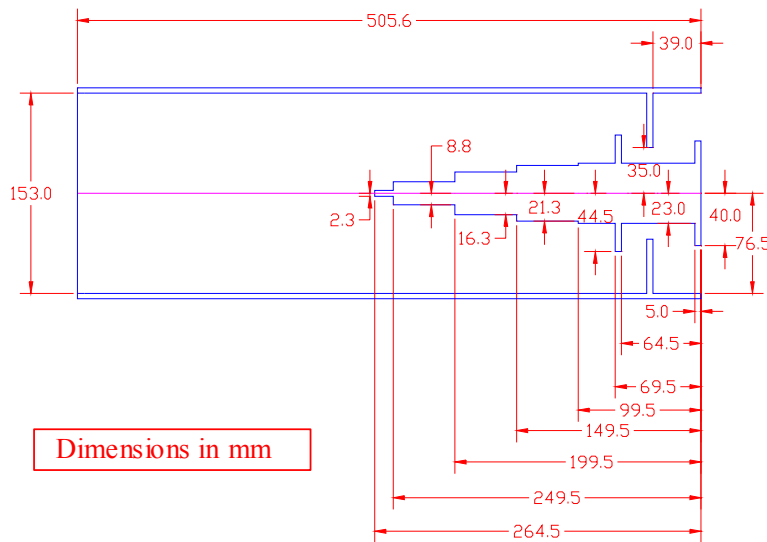


**Figure 3.2 Lovell’s Coaxial Feed Geometry (dimensions in mm)**

<sup>5</sup> T.S. Bird, “Coaxial Feed Array for a Short Focal-Length Reflector”. IEEE Ant and P Symposium, 1997

### 3.2 Second Coaxial and TE<sub>11</sub> Mode Horn Set: 19.0 cm Aperture

#### 3.2.1 TE<sub>11</sub> Mode Feed Horn Geometry

Figure 3.3 shows the geometry of this three-section feed horn. The sections design dimensions were chosen to transition from a 15.3 cm CWG to a 19.0 cm CWG, without generating spurious modes. This design is not optimized in any way and serves as a basis of comparison with the coaxial geometry of both, 19.0 cm and Dr. Bird's 19.6 cm horn design.

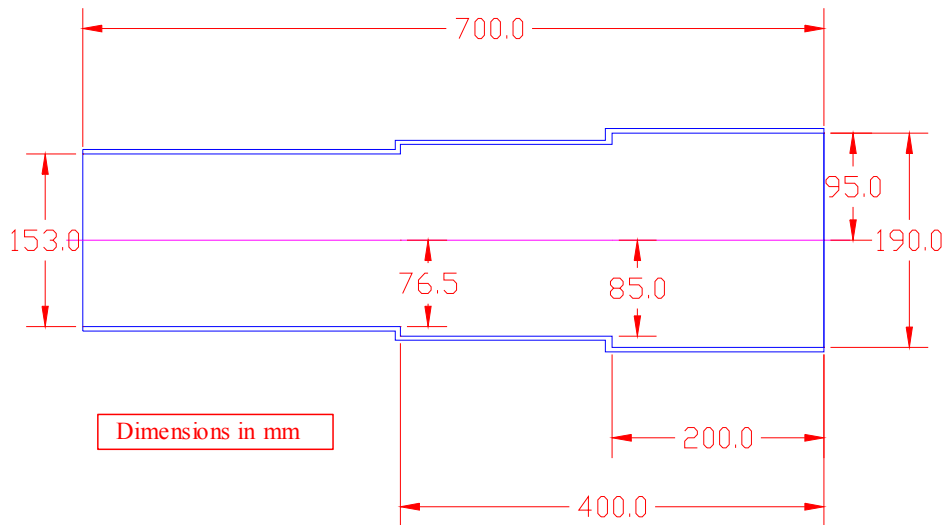


Figure 3.3 TE<sub>11</sub> mode feed Geometry (19.0 cm aperture diameter)

#### 3.2.2 Coaxial Feed Horn Geometry

Figure 3.4 shows the geometry of the 19.0cm diameter coaxial feed. This feed horn was designed, for comparative purposes, based on the previous TE<sub>11</sub> 19.0cm horn, with a multi sectional central transition. Again, no design optimization has been made.

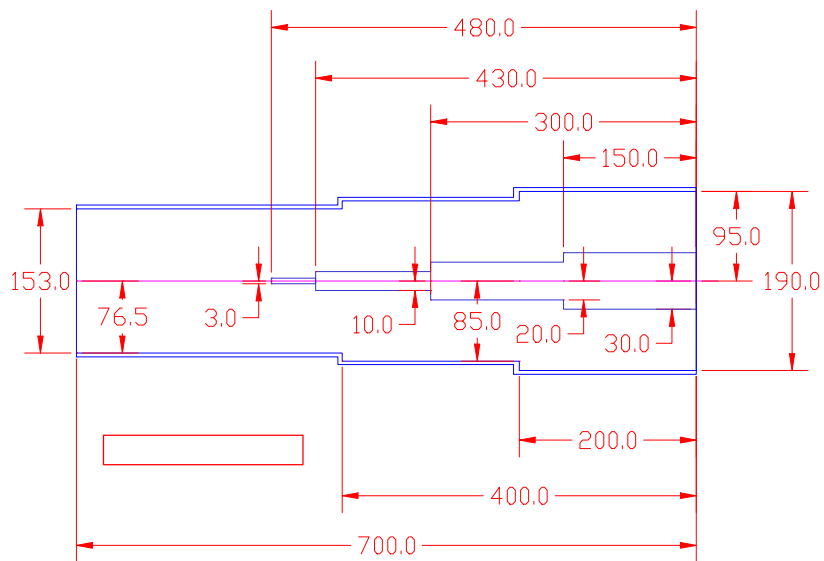


Figure 3.4 Coaxial Feed Geometry (19.0 cm diameter)

### 3.3 Third Coaxial and TE<sub>11</sub> Mode Horn Set

#### 3.3.1 Bird's Coaxial Feed Horn Geometry (19.6 cm Aperture Diameter)

Although there is not geometry available at this time, Dr. Bird's coaxial feed horn has an aperture diameter of 19.6 cm, an irises matching design similar to Lovell's 15.3 cm coaxial horn, and also includes a 60 cm circular plate in the back of the horn to reduce back lobe radiation.

**No Figure  
Available  
at this Time**

**Figure 3.5 Bird's Coaxial Feed Geometry (19.6 cm aperture diameter)**

#### 3.3.2 Parkes TE<sub>11</sub> Mode Feed Horn (24.0 cm Aperture Diameter)

Parkes 24.0 cm TE<sub>11</sub> Mode Feed Horn is a three-section horn, shown in Figure 6.6. The geometry is based on D.B Hayman and T.S. Bird report "*Parkes Multibeam Feed-Horn Measurements*", CSIRO RPP 3803 of November 1995.

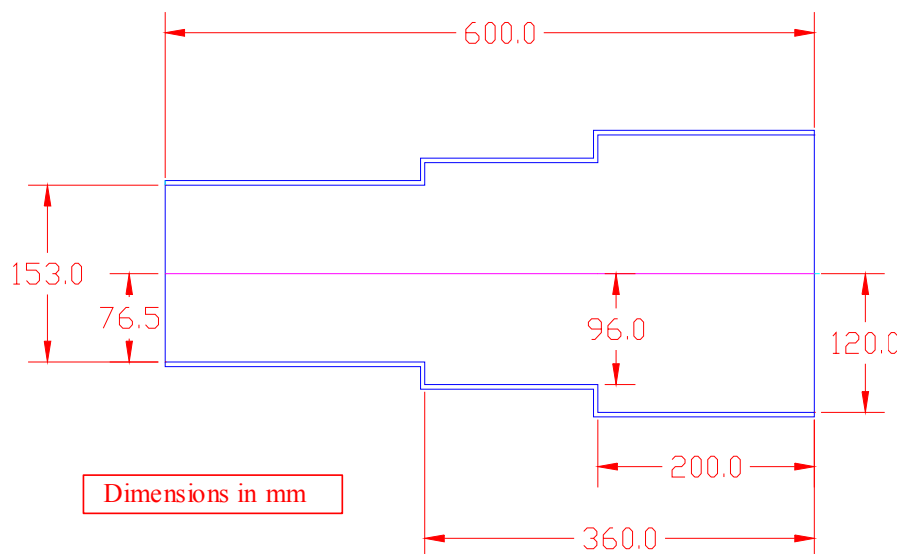


**Figure 3.6 Parkes TE<sub>11</sub> mode feed Geometry (24.0 cm aperture diameter)**

### 3.3.3 TE<sub>11</sub> Mode Feed Horn (26.0 cm Aperture Diameter)

Based on the initial results obtained with these previous horns, (and others including a 28.0 cm aperture TE<sub>11</sub> mode horn not presented here) we designed a 26.0 cm TE<sub>11</sub> mode horn, shown here in Figure 3.7. This horn consists of five sections optimized for matching, with a return loss  $\geq 25$  dB. We found that this particular aperture diameter offers the optimum performance for a TE<sub>11</sub> mode horn array embedded in the Arecibo Gregorian Optics, in terms of aperture illumination and G/T. Arrays with larger horn sizes are dominated by scanning losses.

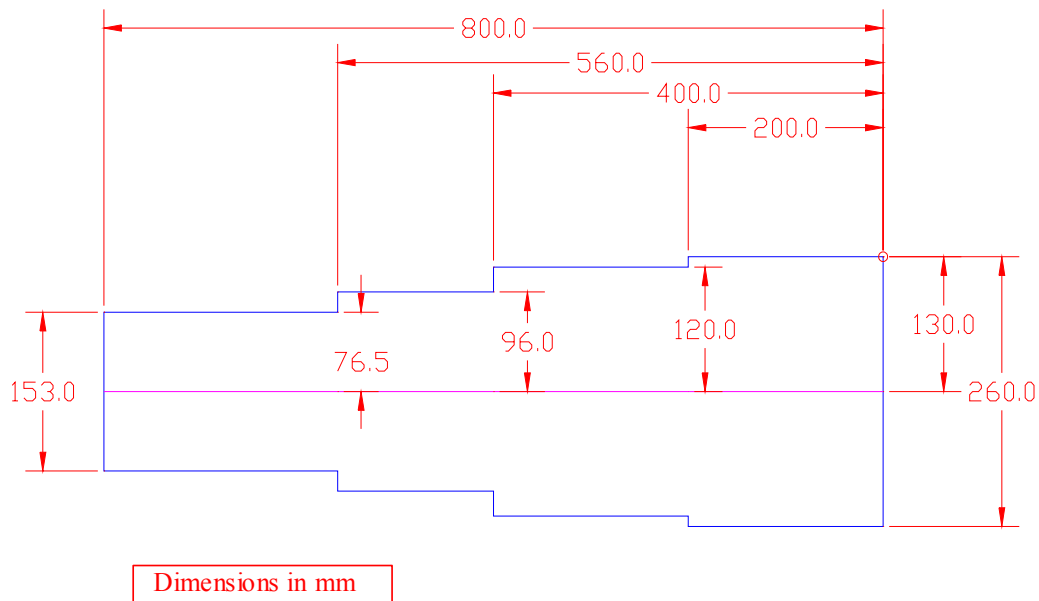


**Figure 3.7 TE<sub>11</sub> mode feed Geometry (26.0 cm aperture diameter)**

## 4. Feed Far Field Radiation Patterns

As It was mentioned earlier, all feed radiation patterns were obtained by a Finite Element full wave analysis of the feed horn structures using Ansoft's HFSS, except for Dr. Bird's coaxial horn, which provided the radiation patterns.

For each horn we are presenting amplitude and phase pattern cuts at the following frequencies: 1.225 GHz, 1.375 GHz, and 1.525 GHz.

Due to the rotationally symmetry of the feeds, only two cuts of the feed's radiation pattern are necessary to analyze the overall antenna performance. Nevertheless, for completeness in this document, an additional cut at  $45^\circ$  is also included here, in the field amplitude figures, to show cross-polar levels.

### 4.1 Radiation Patterns: 15.3 cm Aperture Coaxial and TE<sub>11</sub> Mode Horn Set

#### 4.1.1 TE<sub>11</sub> Mode Horn Far Field Patterns

Figures 4.1 to 4.3 show the far field radiation pattern, magnitude and phase for the TE<sub>11</sub> mode feed with 15.3 cm aperture diameter. The edge taper at  $60^\circ$  is varies from 7.0 to 8.0 dB, and the cross-polar level is better than  $-27$  dB over the band, for  $\theta \leq 60^\circ$ .

#### 4.1.2 Lovell's Coaxial Horn Far Field Patterns

Figures 4.4 to 4.6 show the far field radiation pattern, magnitude and phase for Lovell's coax feed horn with 15.3 cm aperture diameter. The edge taper improves compared with the previous horn, but still  $< 10$  dB. The cross-polar level is better than  $-24$  dB.

**TE<sub>11</sub> mode feed horn (15.3 cm diameter)**

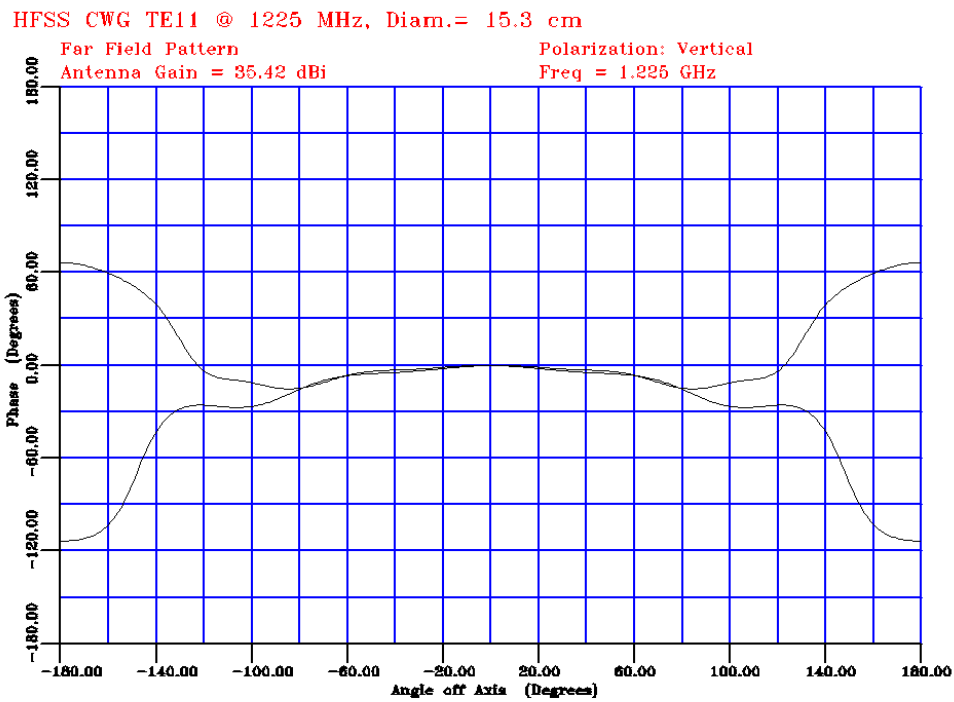
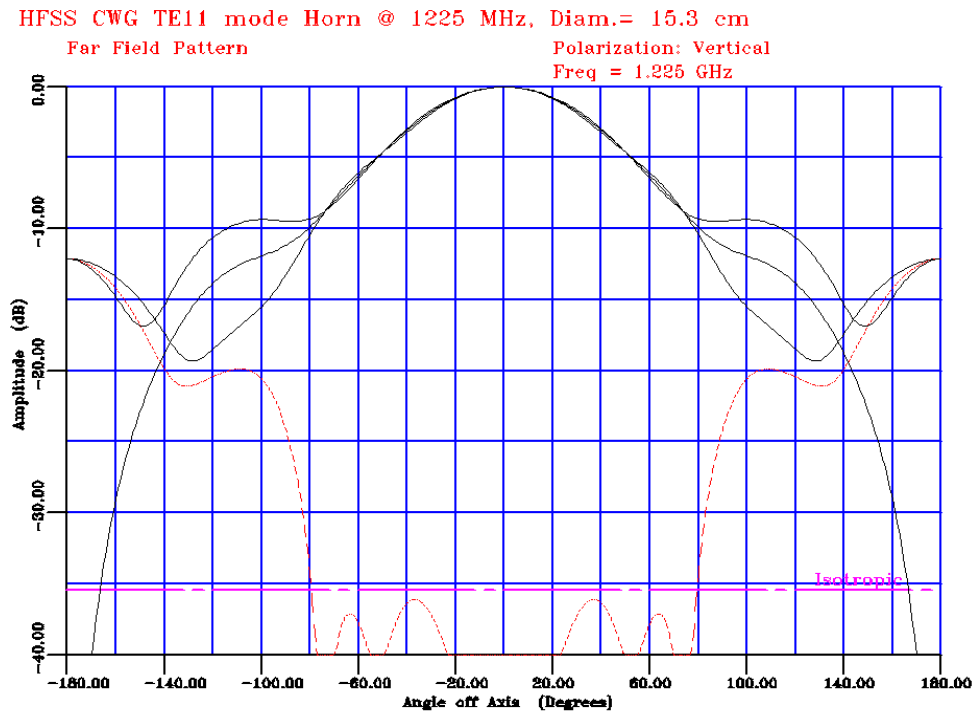


**Figure 4.1 TE<sub>11</sub> mode feed (15.3 cm diameter) Radiation Pattern at 1.225 GHz**

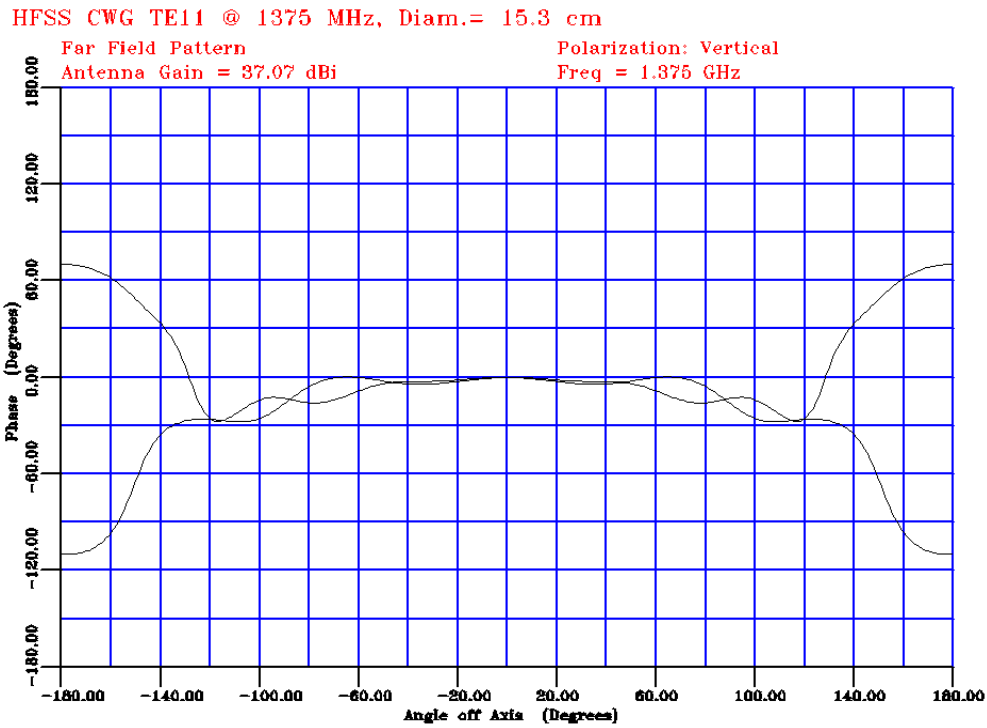
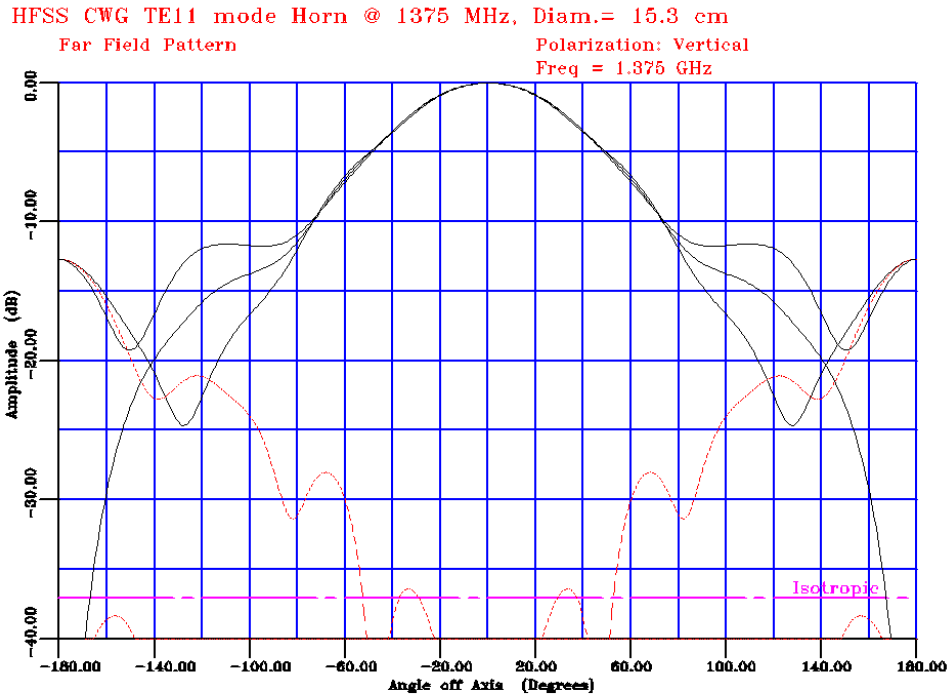


Figure 4.2 TE<sub>11</sub> mode feed (15.3 cm diameter) Radiation Pattern at 1.375 GHz

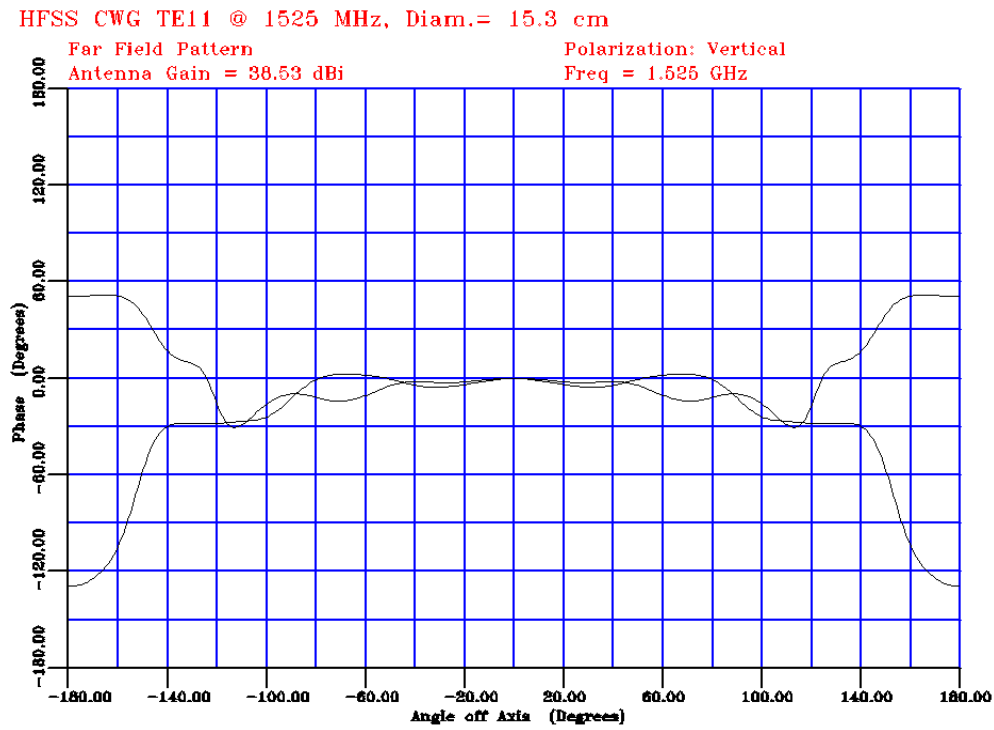
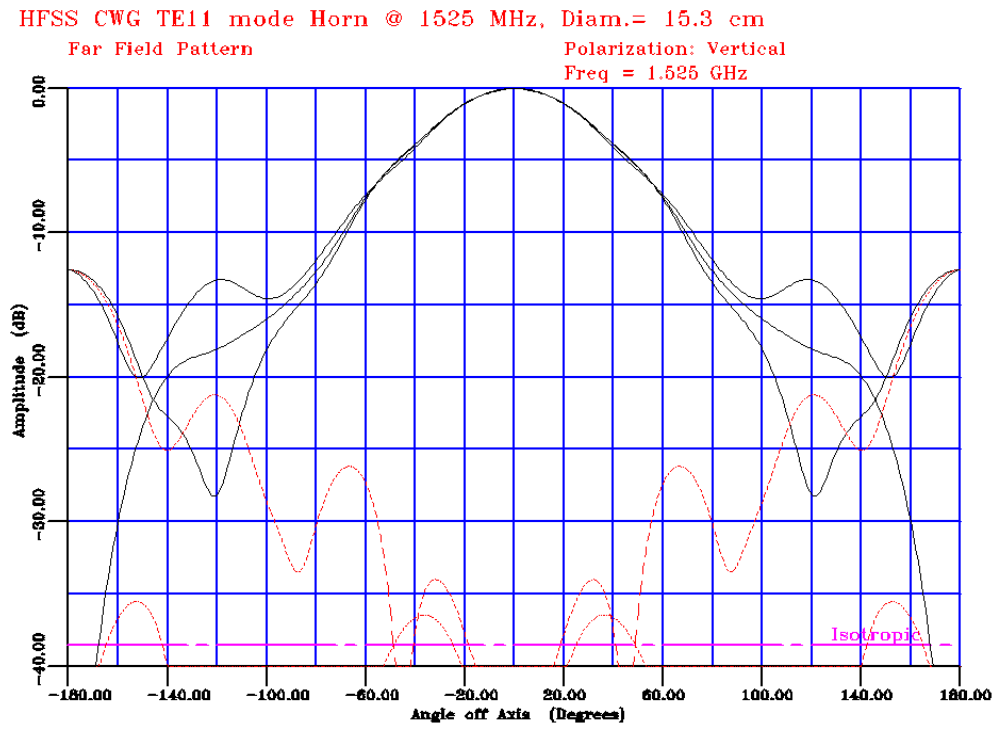


Figure 4.3 TE<sub>11</sub> mode feed (15.3 cm diameter) Radiation Pattern at 1.525 GHz







## **4.2 Radiation Patterns: 19.0 cm Aperture Coaxial and TE<sub>11</sub> Mode Horn Set**

### **4.2.1 TE<sub>11</sub> Mode Horn Far Field Patterns**

Figures 4.7 to 4.9 show the far field radiation pattern, magnitude and phase for the TE<sub>11</sub> mode feed with 19.0 cm aperture diameter. The edge taper approaches now 10.0 dB, with a cross-polar level better than -27 dB. The high frequency pattern (1.525 GHz) has large back-lobes as anticipated for a non-optimized design. This could be overcome by optimizing the horn design.

### **4.2.2 Coaxial Feed Horn Far Field Patterns**

Figures 4.10 to 4.12 show the far field radiation pattern, magnitude and phase for the 19.0cm aperture diameter coax feed. The improvement in the pattern of the coax horn design compared with the TE<sub>11</sub> is evident, although there is a slight difference in the E and H patterns. The edge taper is larger than 10.0 dB starting at 1.375 GHz. The cross-polar levels are better than -26 dB.

TE<sub>11</sub> mode feed horn (19.0 cm diameter.)

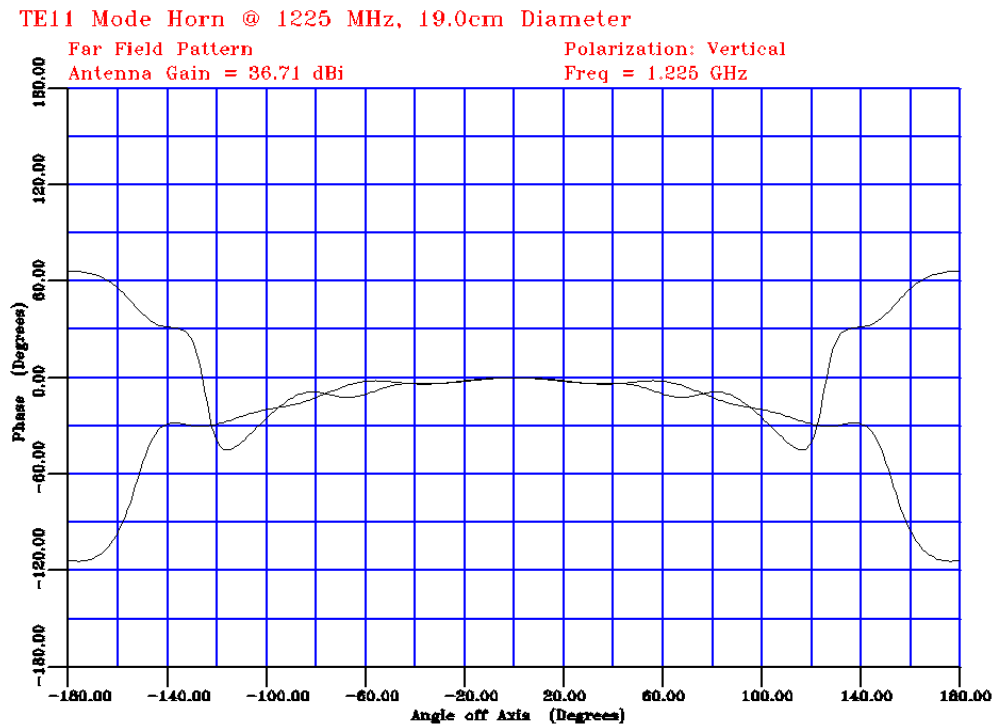
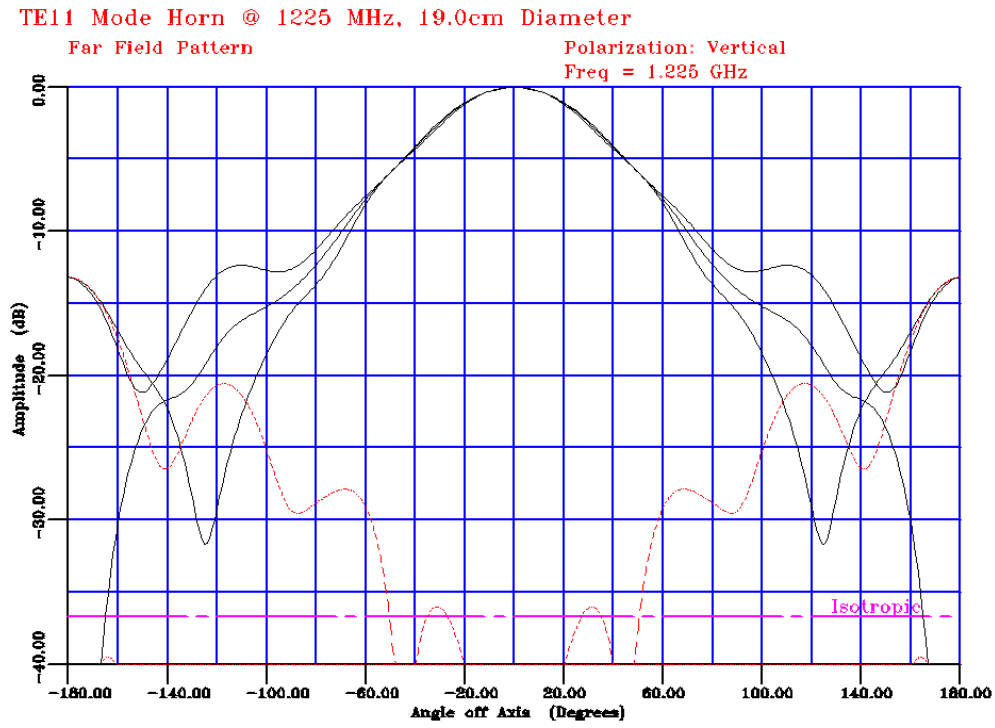


Figure 4.7 TE<sub>11</sub> mode feed (19.0 cm diameter) Radiation Pattern at 1.225 GHz

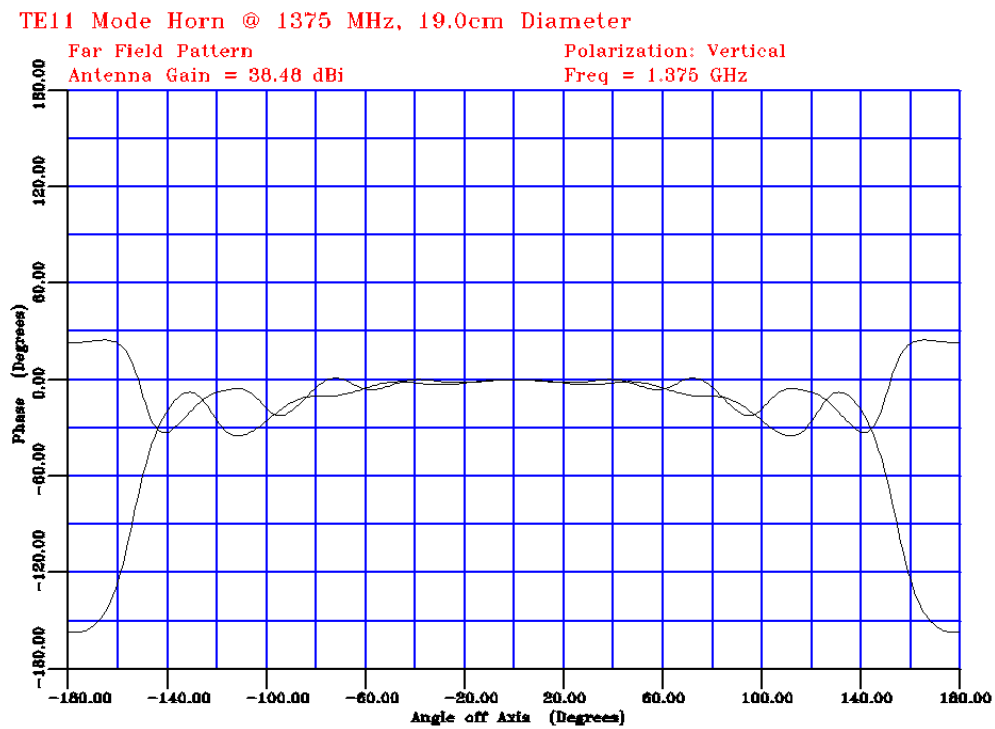
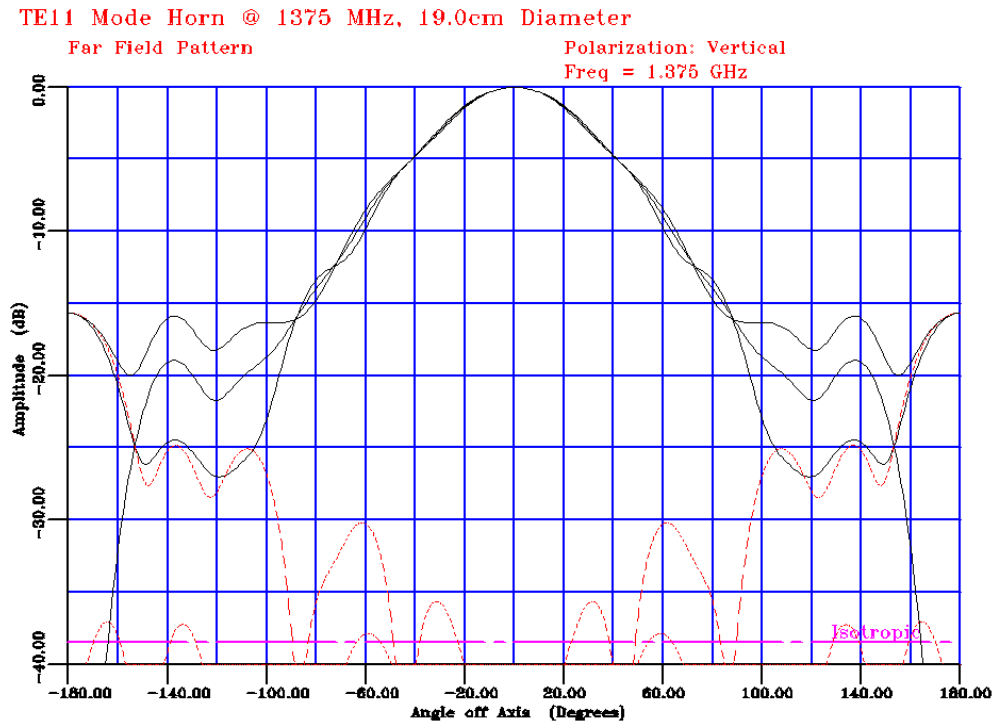


Figure 4.8 TE<sub>11</sub> mode feed (19.0 cm diameter) Radiation Pattern at 1.375 GHz

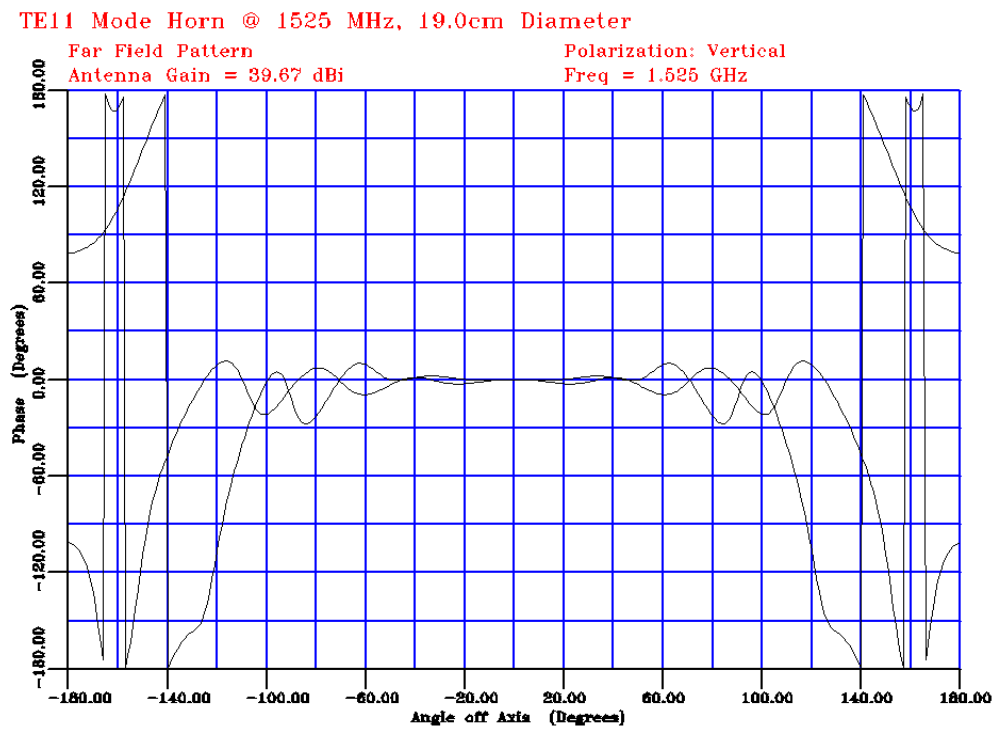
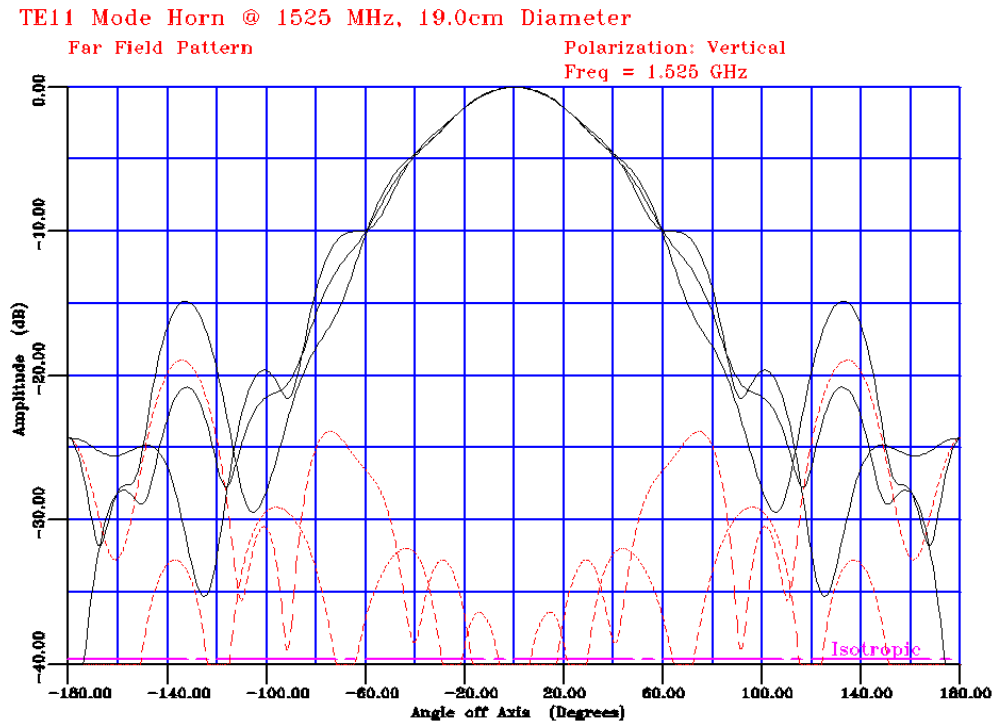


Figure 4.9 TE<sub>11</sub> mode feed (19.0 cm diameter) Radiation Pattern at 1.525 GHz

Coaxial feed horn (19.0 cm diameter.)

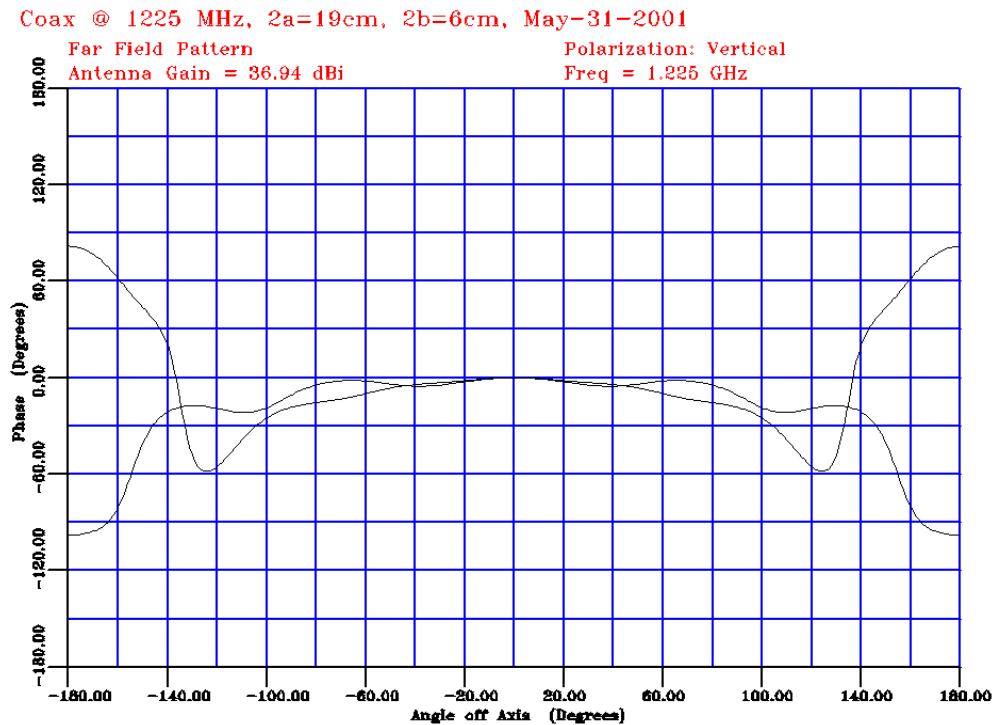
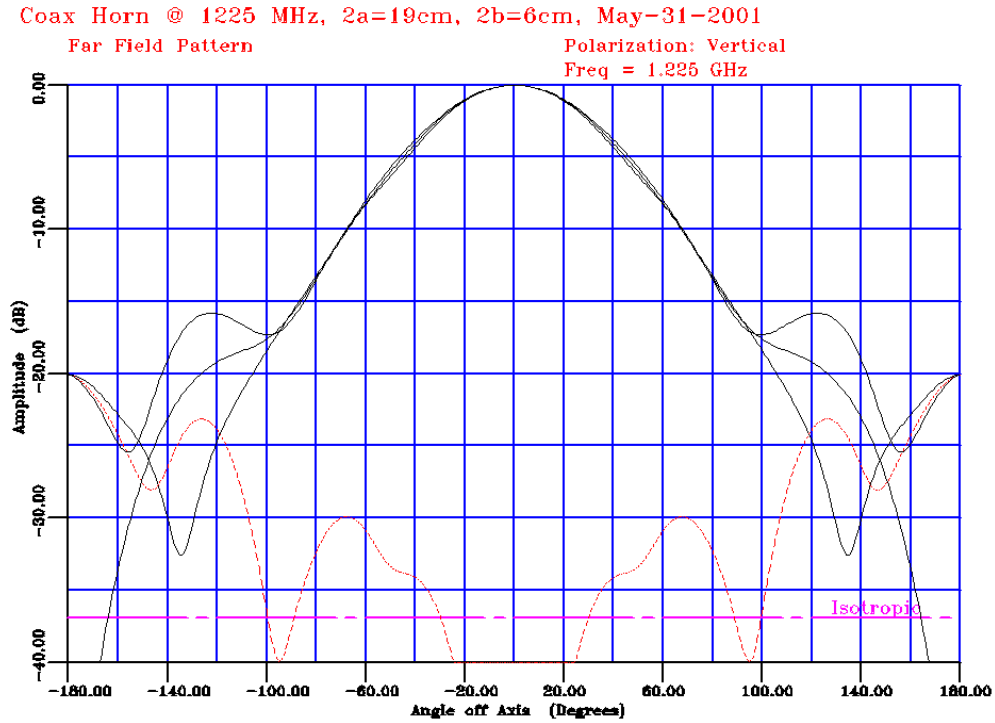


Figure 4.10 Coax feed (19.0 cm diameter) Radiation Pattern at 1.225 GHz

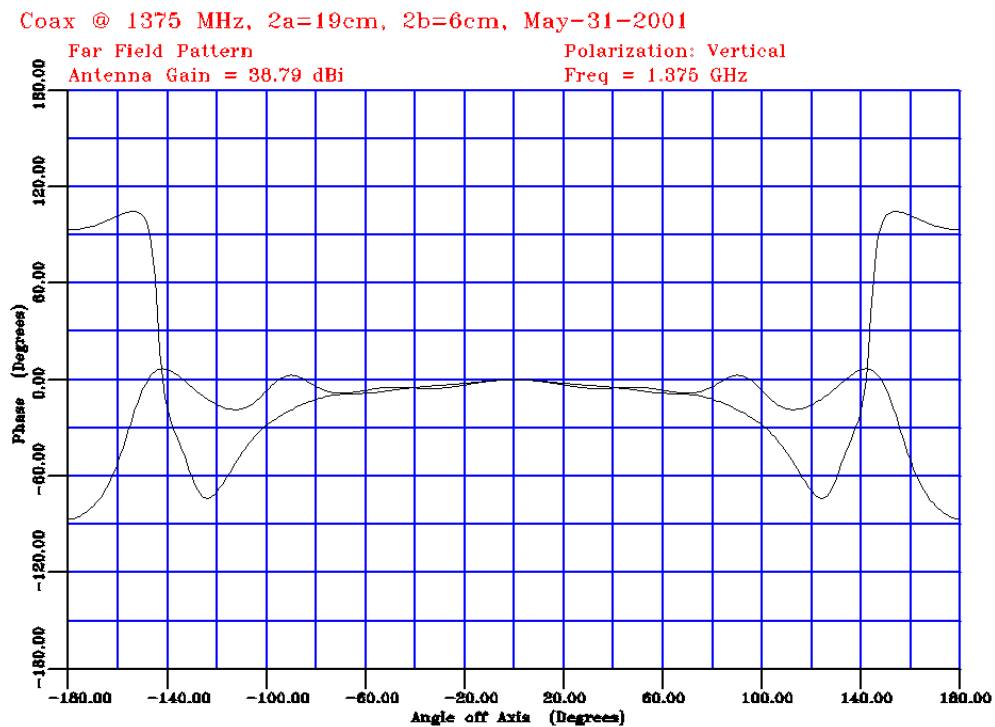
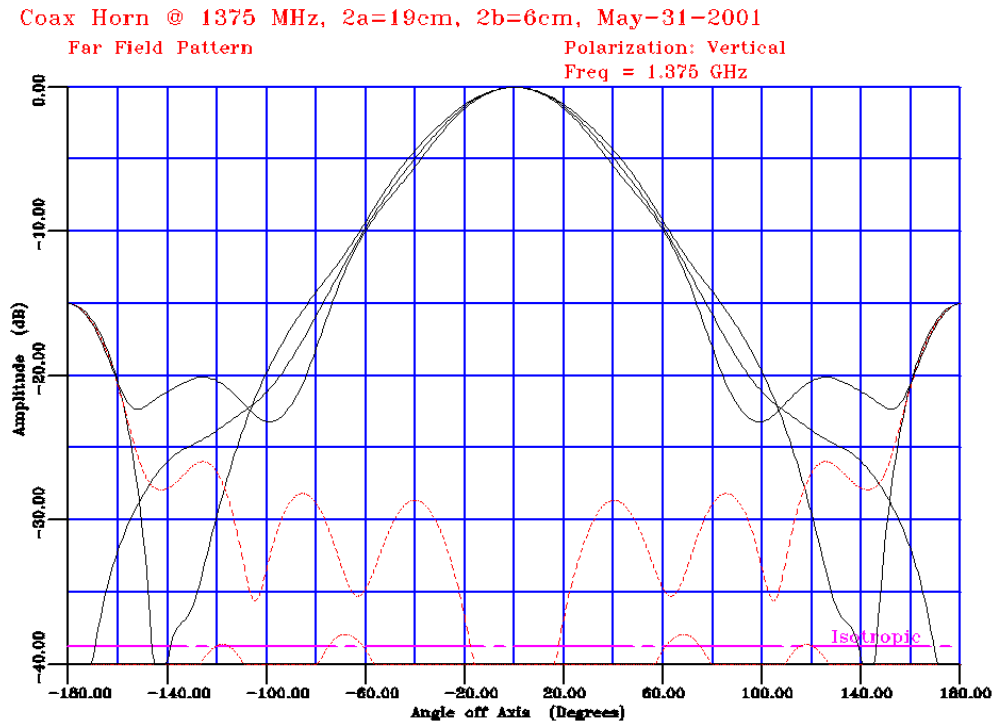


Figure 4.11 Coax feed (19.0 cm diameter) Radiation Pattern at 1.375 GHz

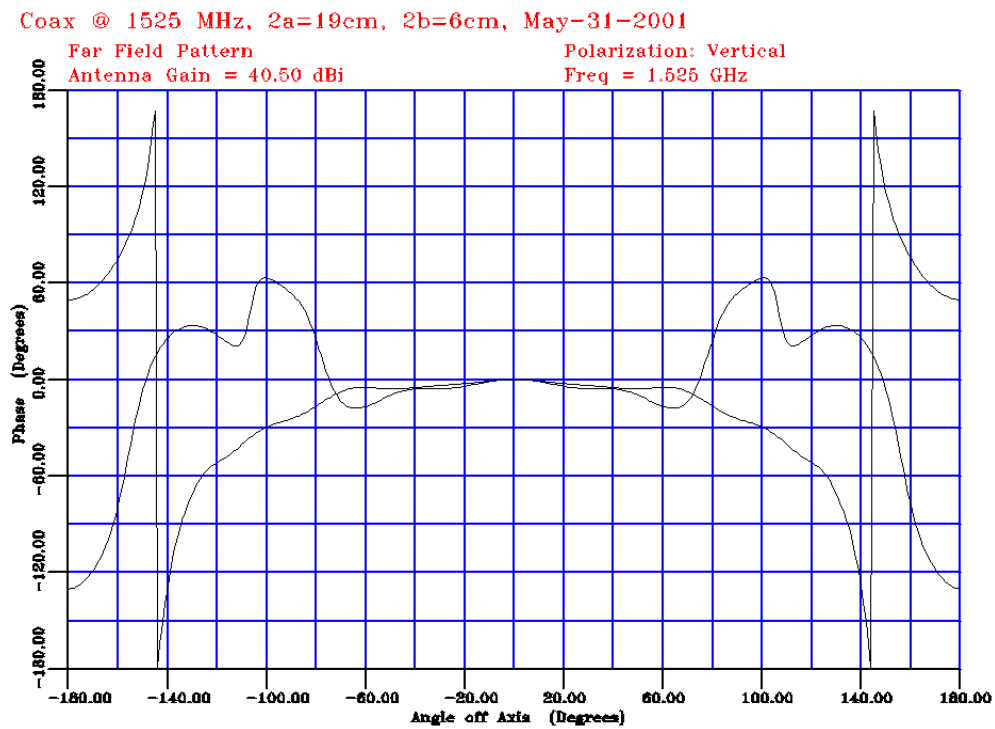
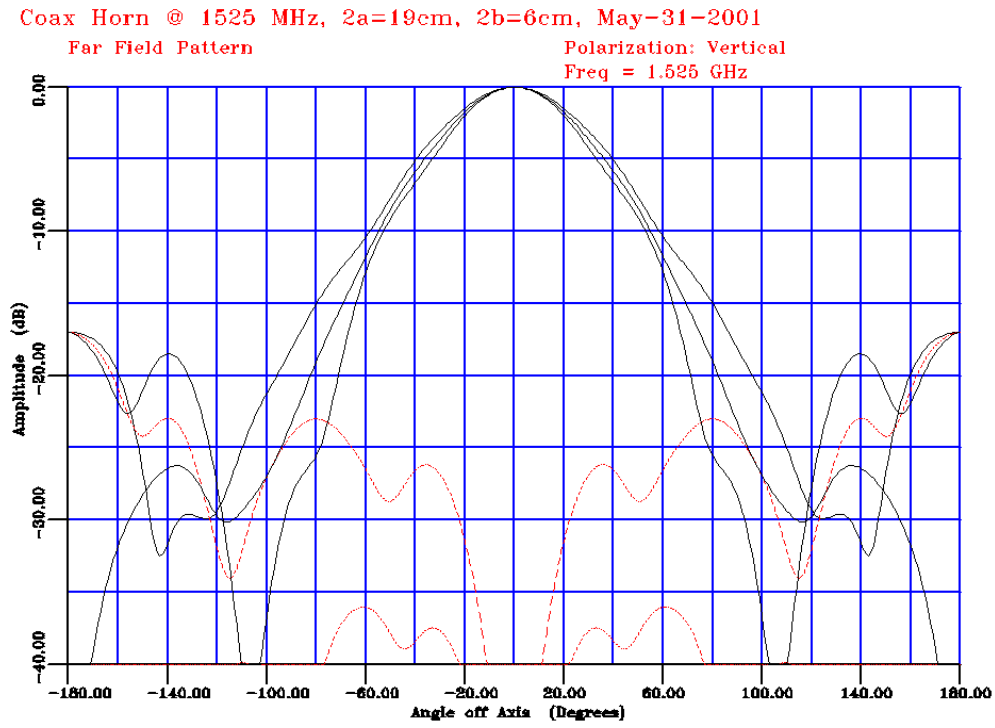


Figure 4.12 Coax feed (19.0 cm diameter) Radiation Pattern at 1.525 GHz

### **4.3 Radiation Patterns: Coaxial and TE<sub>11</sub> Mode Horn Set (Various Apertures)**

#### **4.3.1 Bird's 19.6 cm aperture Coaxial Feed Horn Patterns**

Figures 4.13 to 4.15 show the far field radiation pattern, magnitude and phase for Dr. Bird's coax feed horn with 19.6 cm aperture diameter. Dr. Bird design has an edge taper larger than 10.0 dB starting at 1.475 GHz. The pattern E and H planes are symmetric at the middle frequency only, with a variation from -7 to -10 dB at 1.225 GHz and of -12 to -15 dB at 1.525 GHz. The maximum cross-polar level is better than -23 dB over the band. This horn included a 60 cm diameter back plate to reduce the back lobe radiation, which is evident in the figures.

#### **4.3.2 Parkes 24.0 cm aperture TE<sub>11</sub> Mode Feed Horn Patterns**

Figures 4.16 to 4.18 show the far field radiation pattern, magnitude and phase for Parkes' TE<sub>11</sub> mode feed horn with an aperture diameter of 24.0 cm. The edge taper is larger than 10.0 dB starting at 1.225 GHz and go up to -14 dB at 1.525 GHz. This horn has very low back lobe levels. The cross-polar level of this horn is better than -28 dB over the band.

#### **4.3.3 TE<sub>11</sub> Mode 26.0 cm aperture Feed Horn Patterns**

Figures 4.19 to 4.21 show the far field radiation pattern, magnitude and phase for the 26.0 cm aperture TE<sub>11</sub> mode feed horn. The edge taper is 12.0 dB starting at 1.225 GHz and go up to -17 dB average at 1.525 GHz. This horn has very low back lobe levels. The cross-polar level of this horn is better than -22 dB over the band. The beam is somewhat more asymmetric than Parks horn. The difference between the E and H plane is minimum at the lower frequency, and with -13 to -15 dB variation at mid band, and a variation from -15 dB to -20 dB at 1.525 GHz.

**Dr. Bird's Coaxial feed Horn (19.6 cm diameter.)**

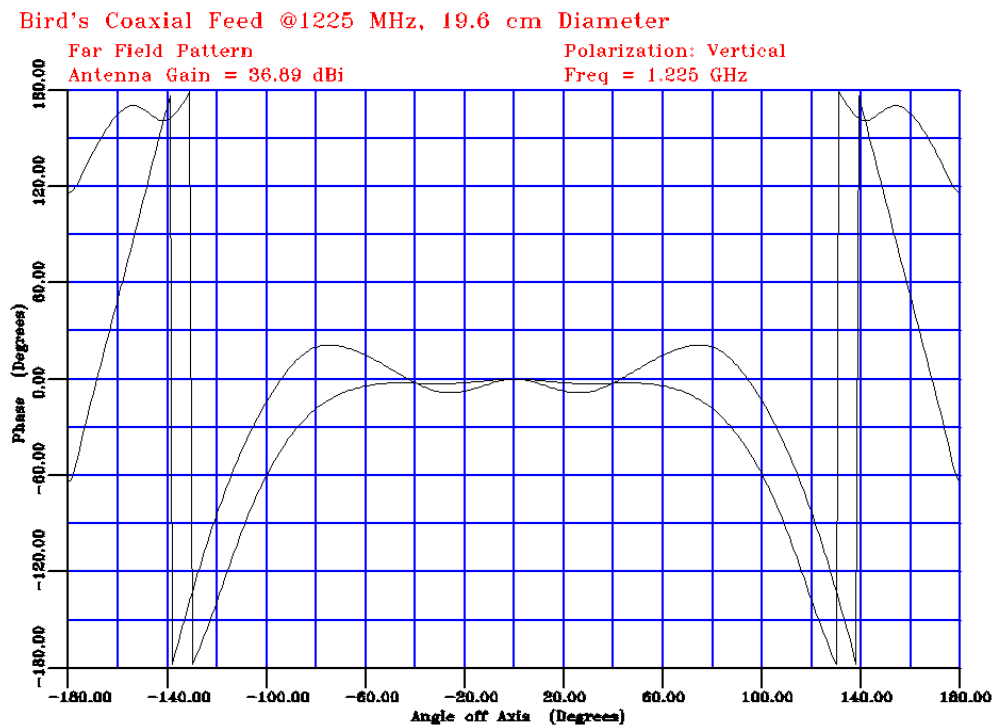
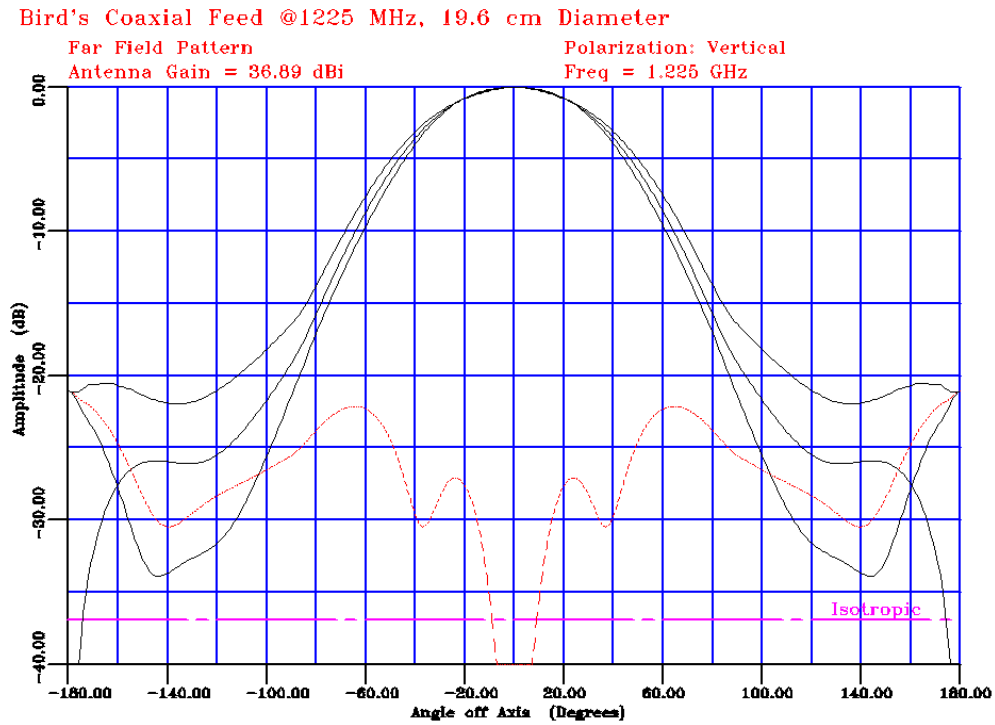


**Figure 4.13 Bird's Coax feed (19.6 cm diameter) Radiation Pattern, 1.225 GHz**

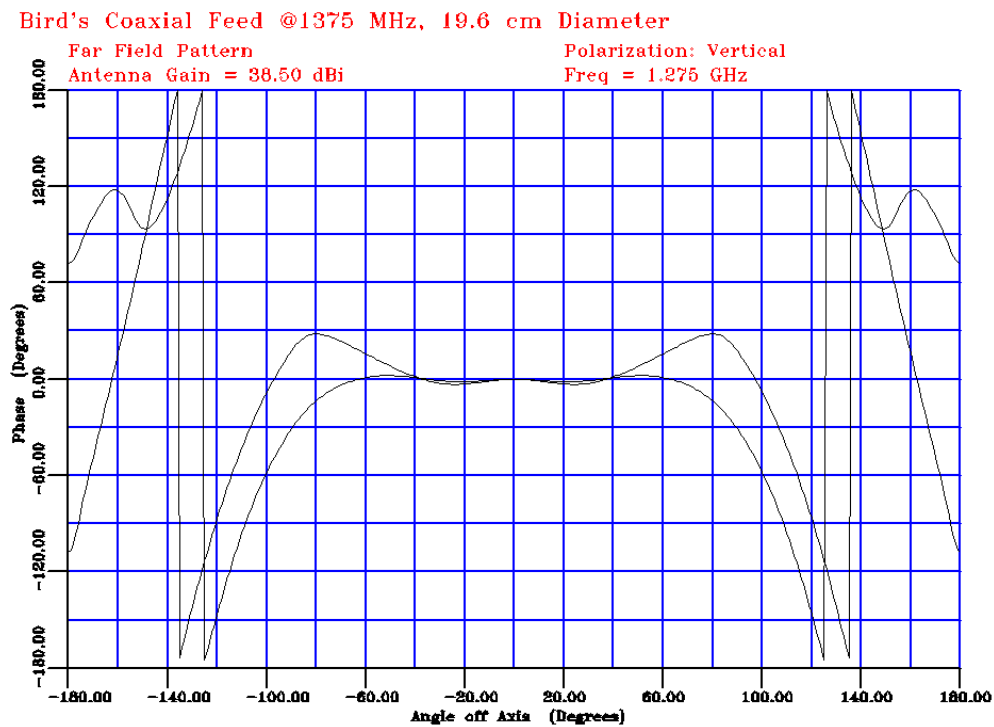
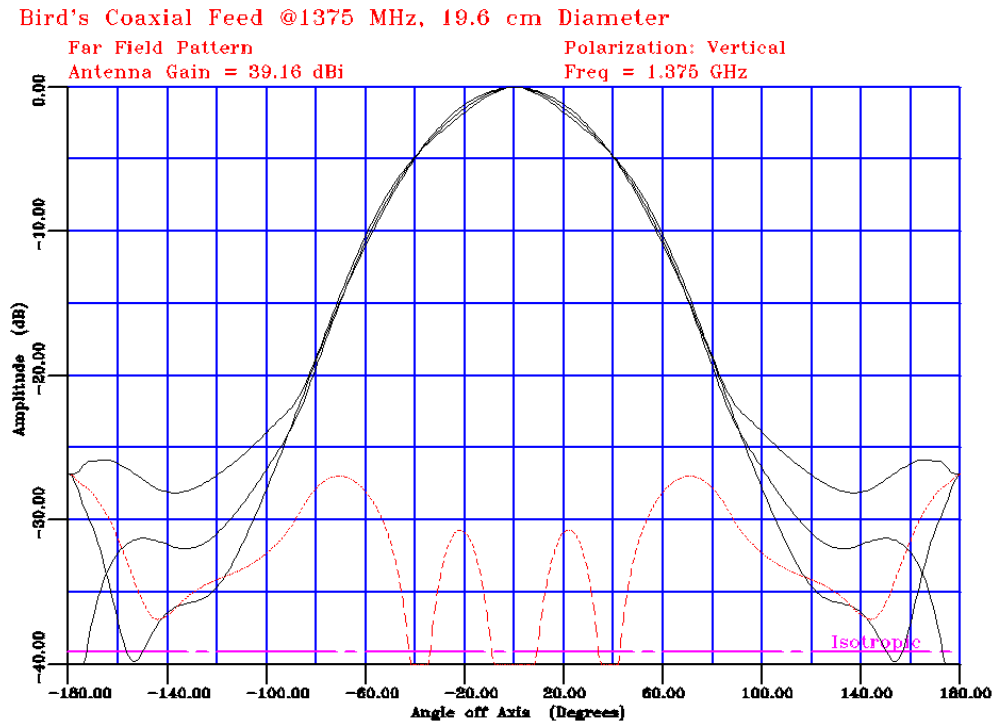


Figure 4.14 Bird's Coax feed (19.6 cm diameter) Radiation Pattern, 1.375 GHz

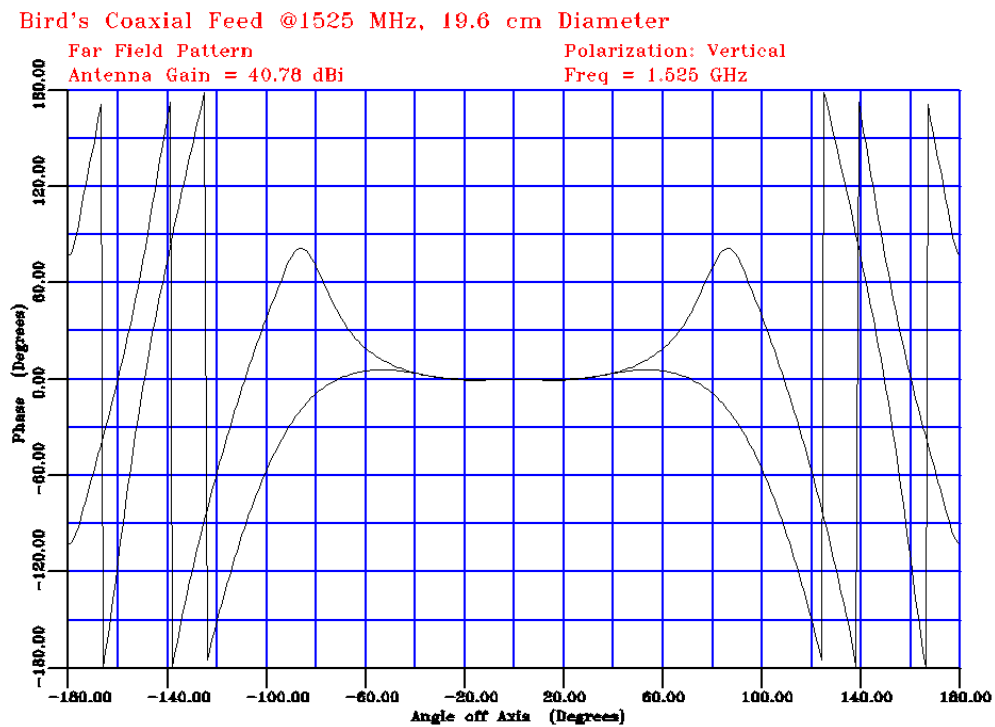
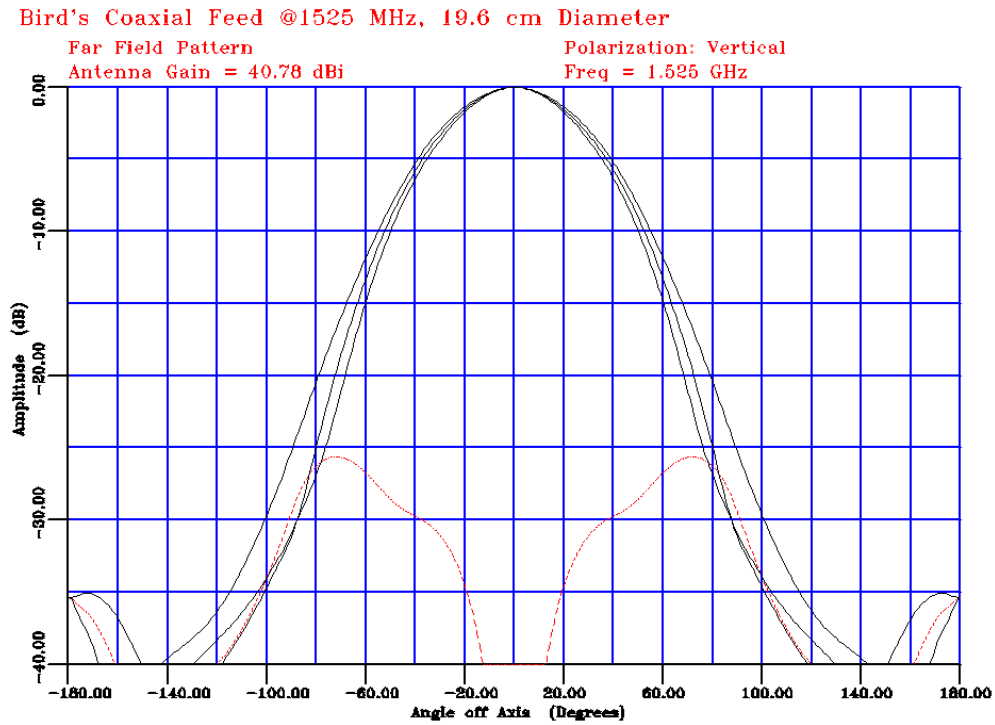
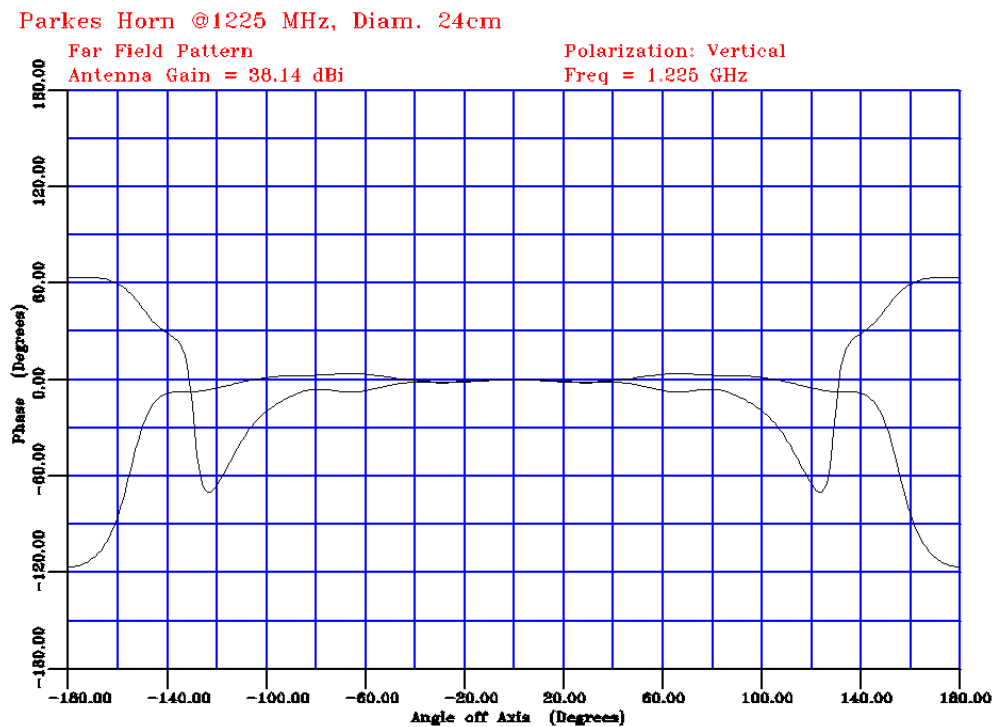
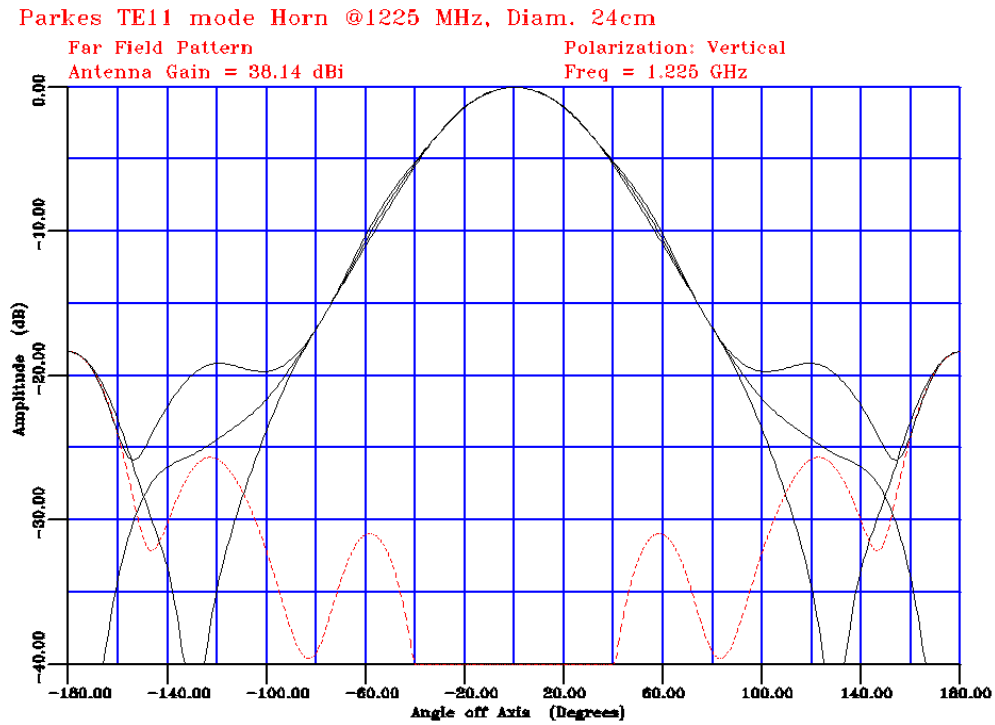


Figure 4.15 Bird's Coax feed (19.6 cm diameter) Radiation Pattern, 1.525 GHz

**Parkes TE<sub>11</sub> mode feed horn (24.0 cm diameter.)**



**Figure 4.16 Parkes TE<sub>11</sub> feed (24.0 cm diam) Radiation Pattern at 1.225 GHz**

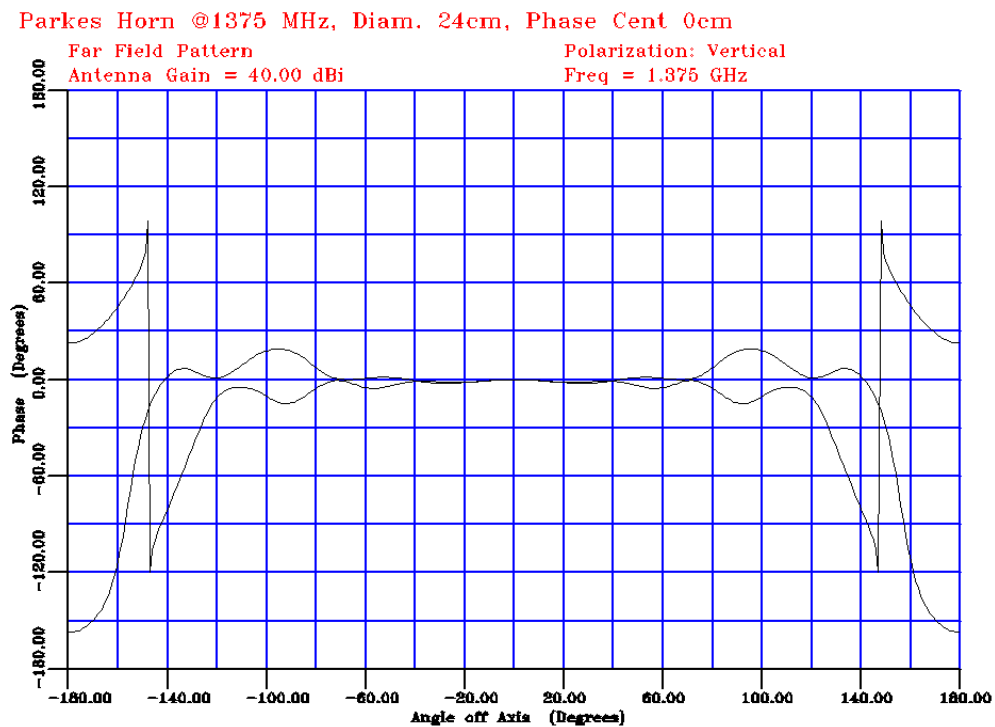
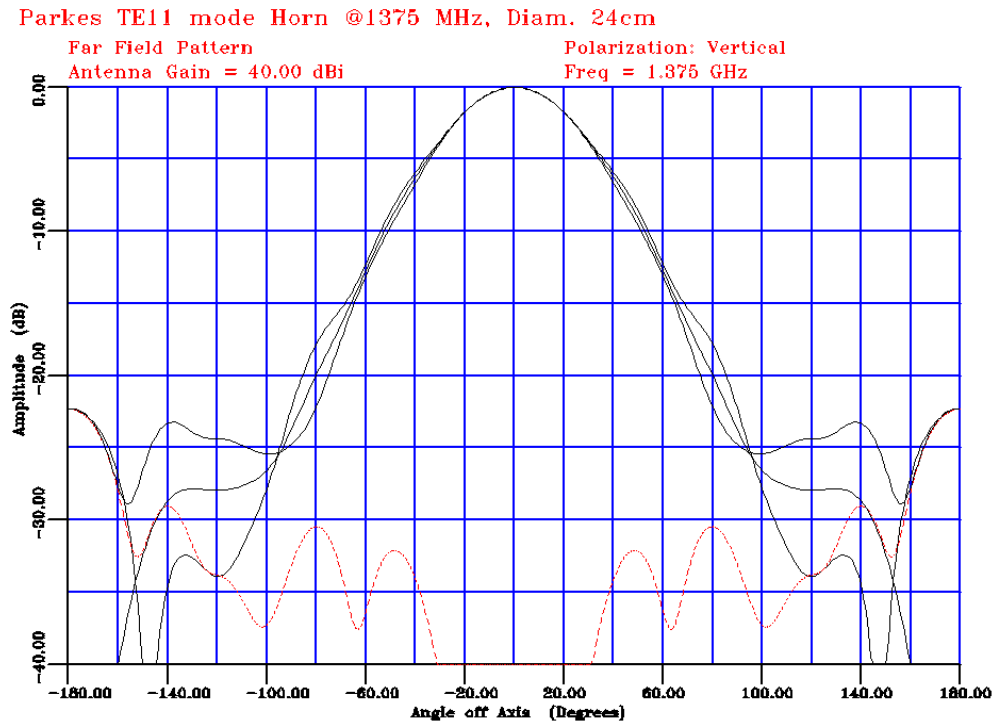


Figure 4.17 Parkes TE<sub>11</sub> feed (24.0 cm diam) Radiation Pattern at 1.375 GHz

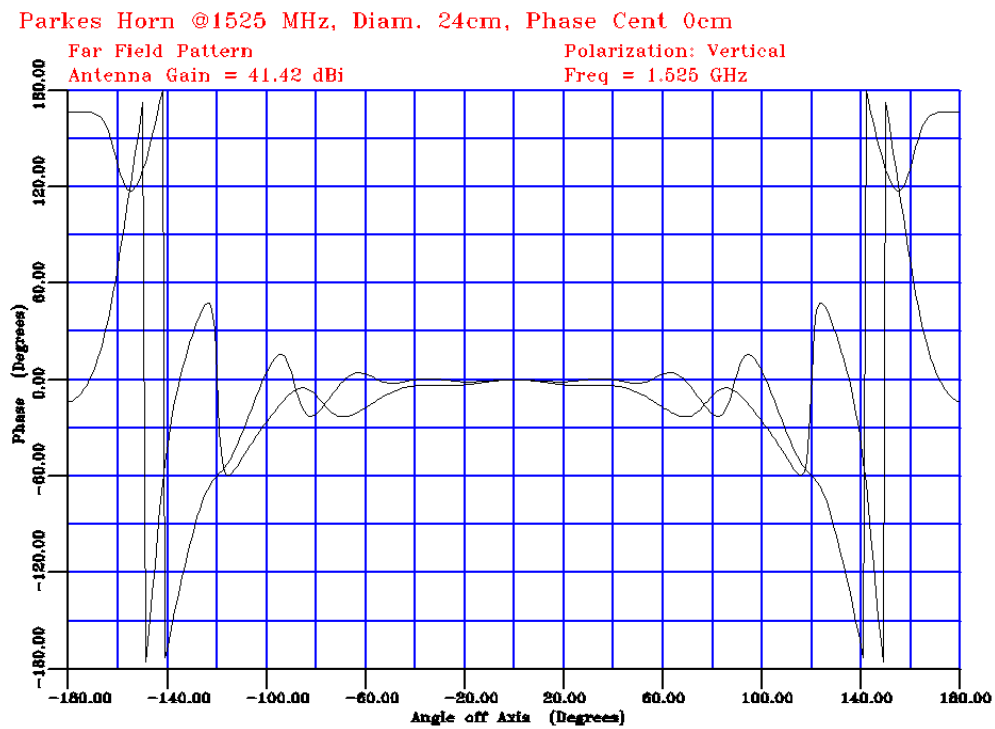
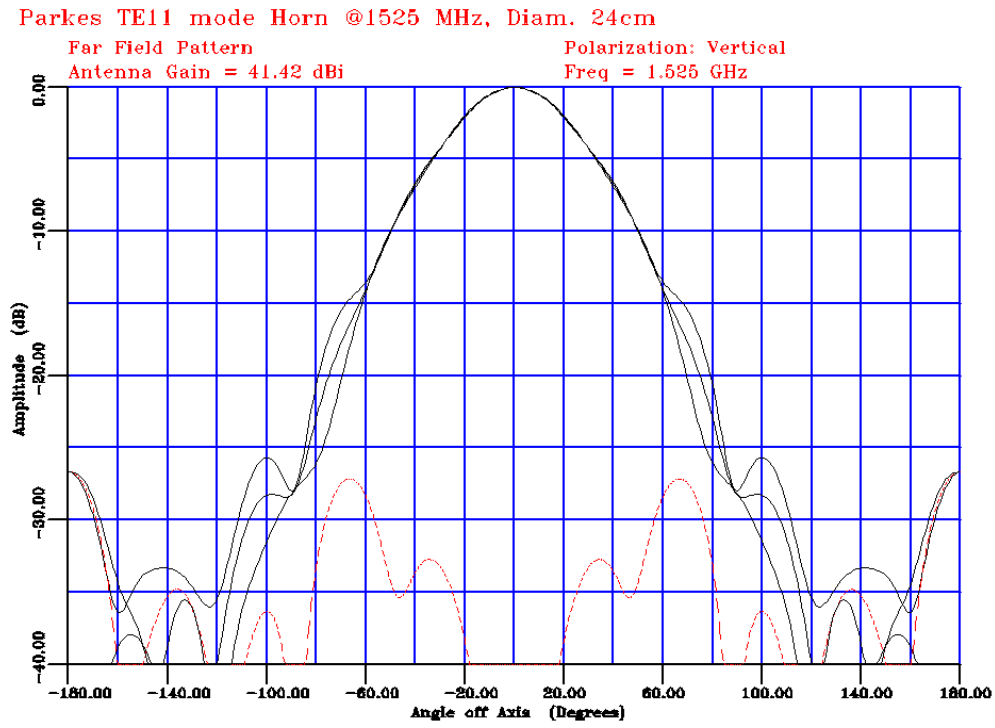
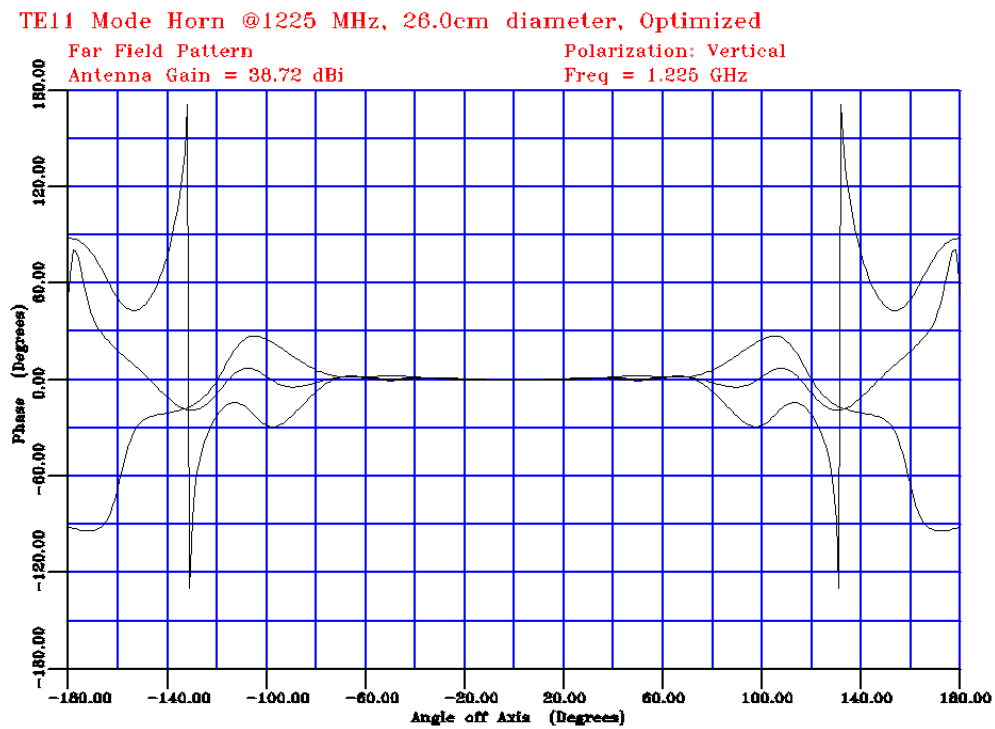
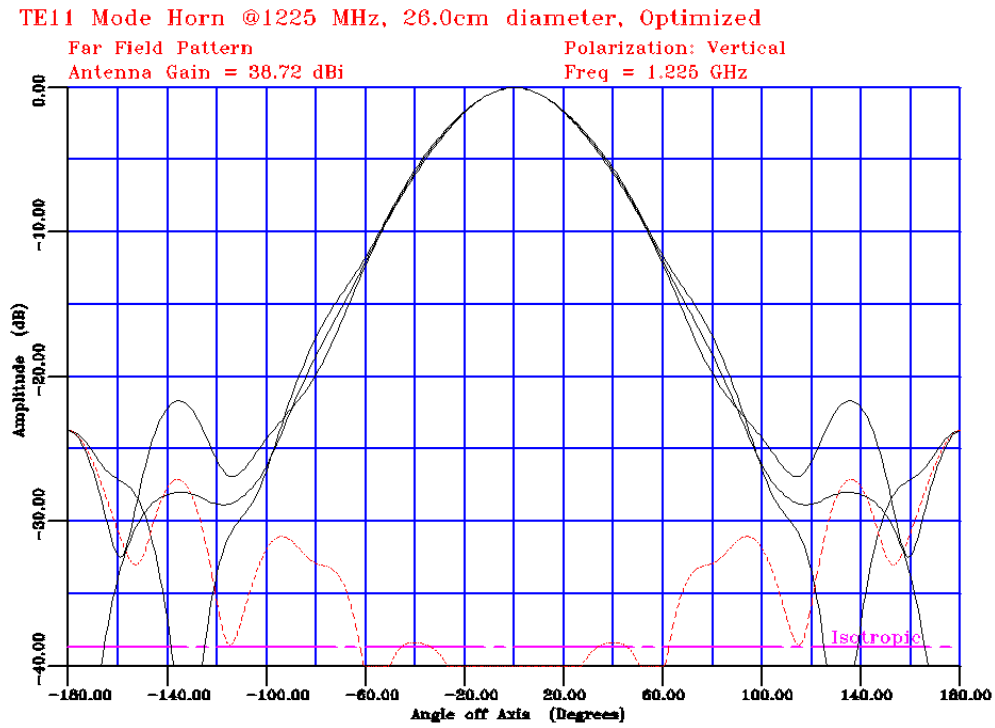


Figure 4.18 Parkes TE<sub>11</sub> feed (24.0 cm diam) Radiation Pattern at 1.525 GHz

**TE<sub>11</sub> mode feed horn (26.0 cm diameter.)**



**Figure 4.19 TE<sub>11</sub> Mode Horn (26.0 cm diam) Radiation Pattern at 1.225 GHz**

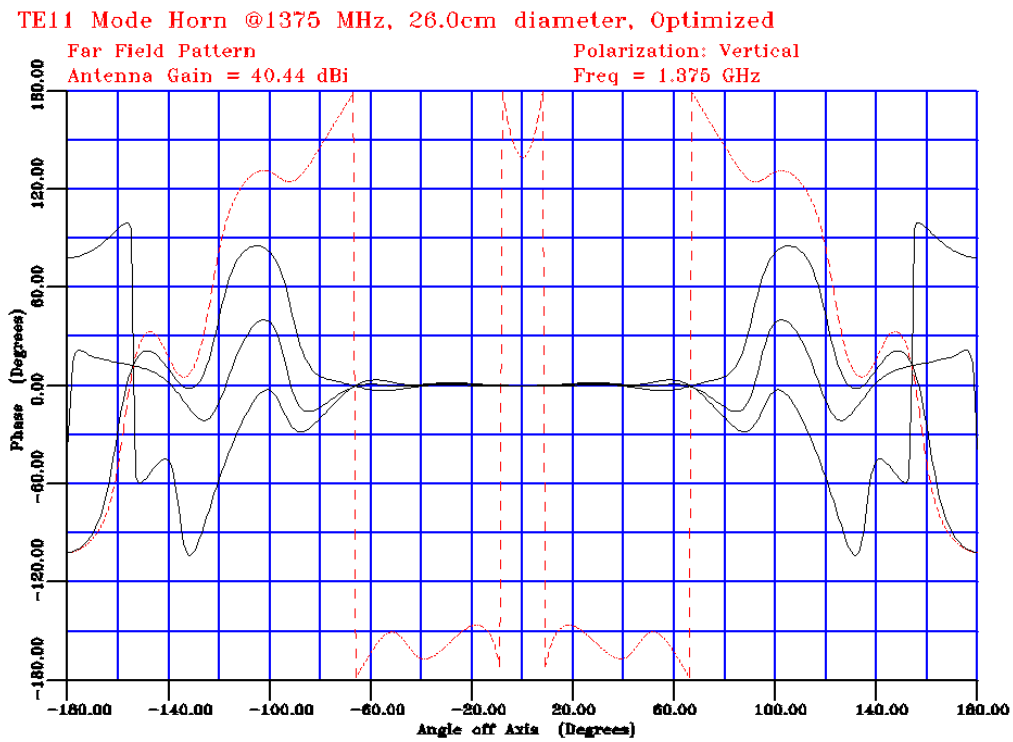
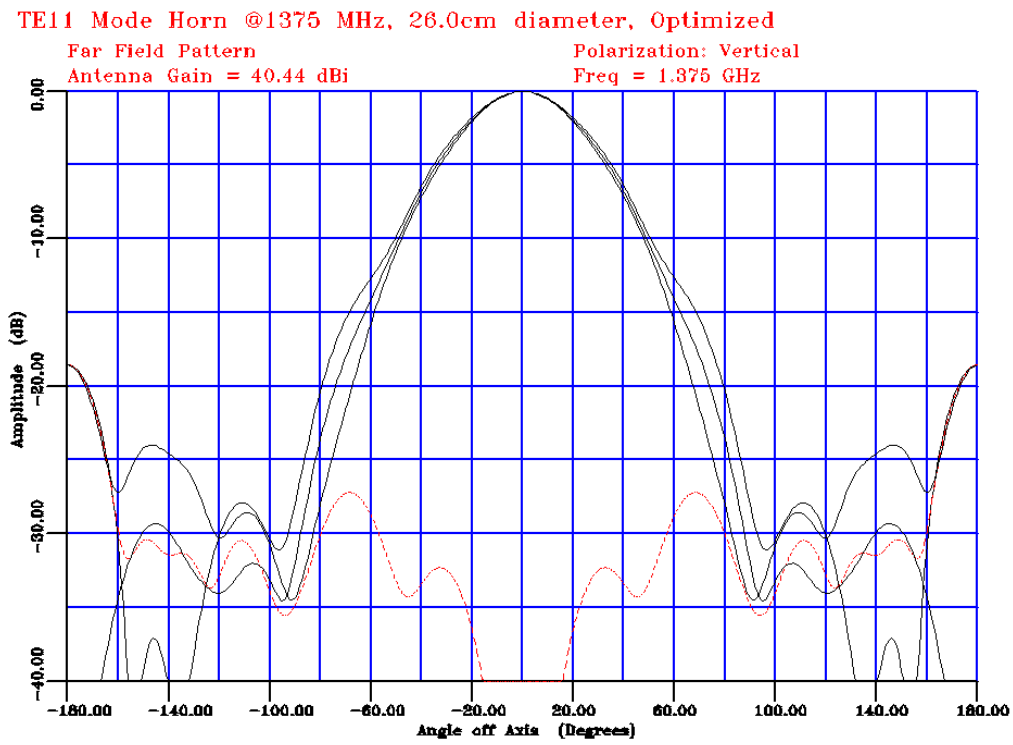


Figure 4.20 TE<sub>11</sub> Mode Horn (26.0 cm diam) Radiation Pattern at 1.375 GHz



## 4.4 Discussion

The following preliminary conclusions may be drawn from the pattern cuts:

- Coaxial horns have lower side lobe levels than TE<sub>11</sub> mode horns with the same aperture diameter.
- Coaxial horns have higher cross-polar component compared with TE<sub>11</sub> mode horns with the same aperture diameter.
- TE<sub>11</sub> mode horns tend to have less variation between E and H plane beam widths than coaxial horns with the same aperture diameter.
- The 60 cm back plate on Dr. Bird's 19.6 cm coaxial horn reduces noticeably the back lobe radiation.
- Edge taper larger than 10 dB at 60° are obtained with apertures  $\geq 24.0$  cm.
- Coaxial horns have larger phase errors (of the order of 15° to 25°) compared with TE<sub>11</sub> mode horns in general (2° to 5°). The 24.0 cm and 26.0 cm TE<sub>11</sub> mode horns, have very small phase errors at 1.225 and 1.375 GHz, nevertheless, at 1.525 GHz, they have phase errors of the same order as the coaxial horns.

## 4.5 What About Input Matching?

Another relevant question for the horns is input matching. Although, it is possible to match the feed in the OMT section, is preferable to have a separate match designs for the horn section and OMT since their purpose is different. In that regard is important to have a good match in the launcher section of the horn. For fractional bandwidths of  $\Delta f/f=22\%$  such as the present one, is particularly difficult to match the lower edge of the frequency band given that is too close to cutoff.

Since information about the horn geometry is not available for all the horns, we are going to compare only two cases: the 15.3 cm TE<sub>11</sub> mode and coaxial horn set, and Parkes, 24.0 cm, and the 26.0 cm TE<sub>11</sub> mode horns.

The input matching with just the 15.3 TE<sub>11</sub> mode circular waveguide into open air, shown in Figure 4.22, is very poor with return losses of 7.0 dB or better over the band. On the other hand, Lovell's coaxial design has better matching, although, their frequency specifications were different, i.e., from 1.33 GHz to 1.43 GHz, return losses are better than 22. dB over their frequency band. The combined inductive and capacitive irises used for matching this coaxial horn, along with stepping down the center conductor, allows for a 10 to 15% matching bandwidth feasible.<sup>6</sup>

Figure 4.23 shows the input matching of Parkes 24.0 cm TE<sub>11</sub> mode horn and of our 26.0 cm TE<sub>11</sub> mode horn. The input matching obtained in our simulation of Parkes horn is better than -14 dB over its specified frequency band (1.270 GHz to 1.470 GHz). Although, a return loss better than 17 dB is reported<sup>7</sup>, the overall shape of the return loss curve agrees with our simulation. In the same graph, we show the matching of our

<sup>6</sup> T.S. Bird, G.L. James & S.J. Skinner, "Input mismatch of TE<sub>11</sub> mode coaxial waveguide feeds", *IEEE Trans. Antennas and Propagation*, vol. 34, pp. 1030-1033, 1986.

<sup>7</sup> T.S. Bird, "A Multibeam Feed for the Parkes Radio-Telescope", *IEEE Antennas and Prop. Symposium, USA, 19-24 June, 1994*.

optimized, five-section, 26.0 cm TE<sub>11</sub> mode horn, with return losses better than 25 dB from 1.20) GHz to 1.550 GHz.

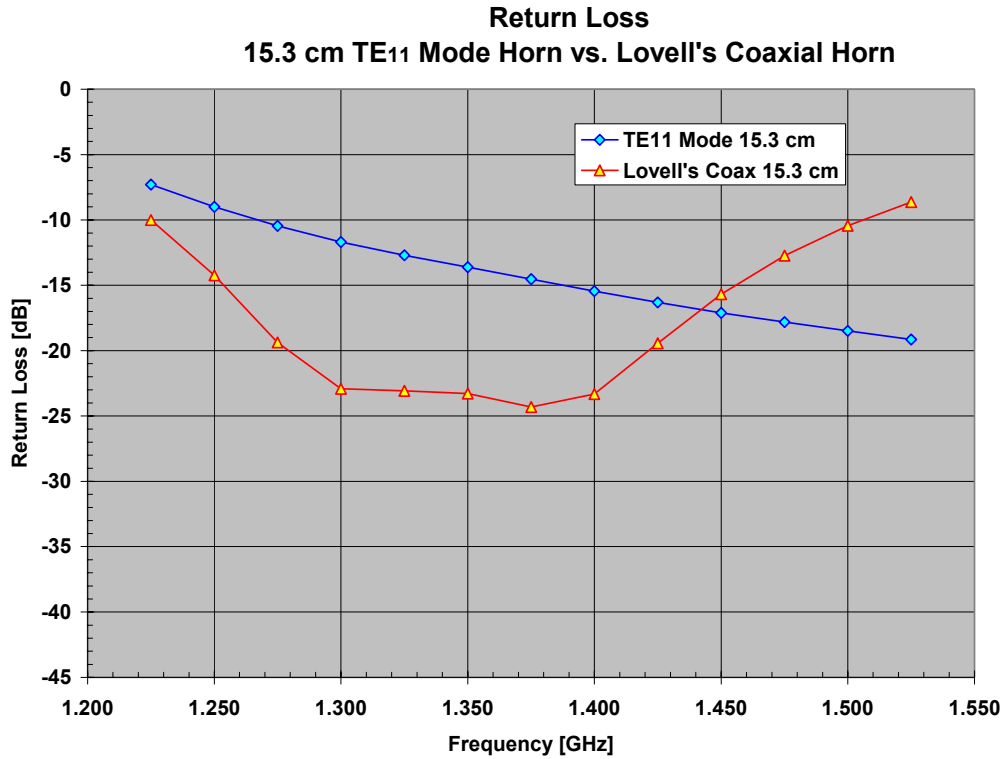


Figure 4.22 Matching characteristics of 15.3 cm Lovell’s coaxial and TE<sub>11</sub> Mode Horn

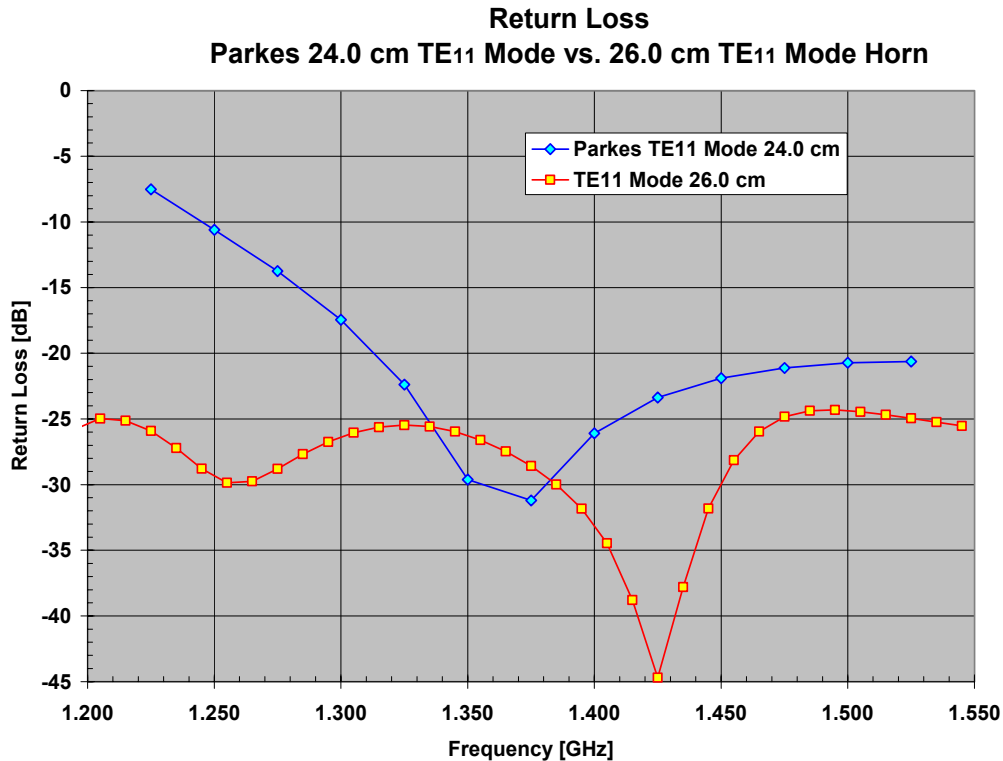


Figure 4.23 Matching characteristics of Parkes 24.0 cm and 26.0 cm TE<sub>11</sub> Mode Horns

## 5. Multibeam Array Layout and Field of View

### 5.1 Arecibo Gregorian System Optics

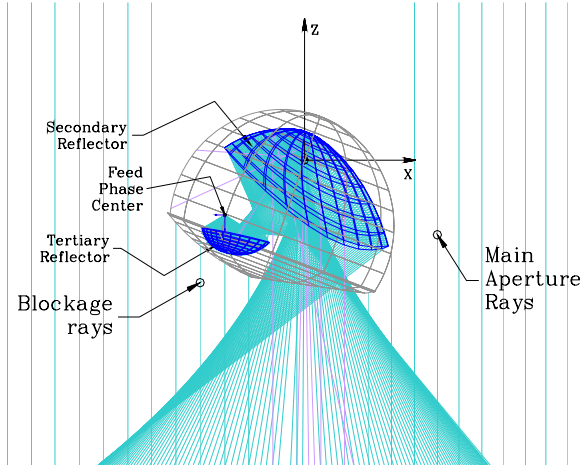


Figure 5.1 General Optical Layout

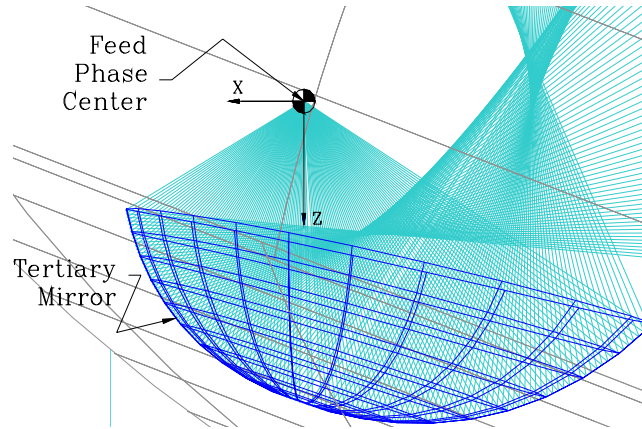


Figure 5.2 Optical Layout Detail

Figure 5.1 shows a general overview of the secondary and tertiary mirror optics of the Arecibo Gregorian system including some ray traces of the optical path. Figure 5.2 shows a detail of the tertiary mirror and coordinate system associated with the feed horn phase center. In particular notice the asymmetry of the optical path as well as the direction of the x-axis and z-axis<sup>8</sup> at the phase center.

### 5.2 Feed Array Geometry

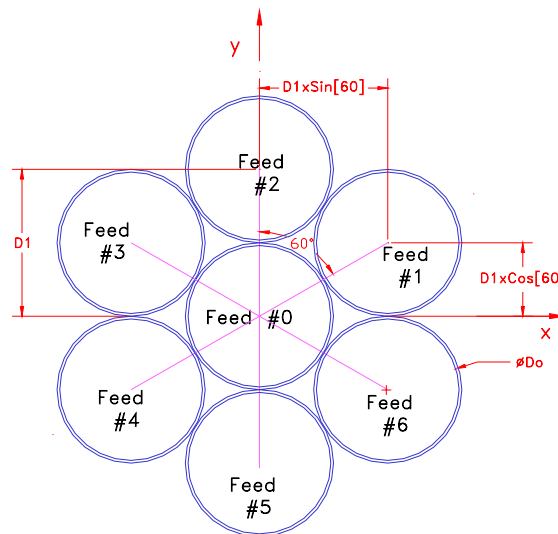


Figure 5.3 Array Layout in the Focal Plane

<sup>8</sup> Notice that the antenna main coordinate system is centered at the apex of the main caustic, pointing upwards in Figure 5.1, while the feed local coordinate system points downwards, (Figure 5.2)

Figure 5.3, shows the front view of the array indicating pixel nomenclature and location.  $D_0$ , and  $D_1$ , in the Figure indicate the feed aperture diameter and the feed center-to-center distance for the array respectively.

We assumed a wall thickness of  $\Delta t=4\text{mm}$ , for the feed horns analyzed, therefore,  $D_1 = D_0 + 2x\Delta t$ .

Due to the mirror symmetry of the optics of the Arecibo Gregorian System, only Feed #0, Feed #1, Feed #2 and Feed #3 need to be analyzed, from which the performance of Feed #4, #5 and #6 can be inferred.

### 5.3 Field of View and Scanning Losses

The scanning losses in the focal plane of the Arecibo Gregorian System at 1.375 GHz. are shown in Figure 5.4. This graph was obtained by displacing an ideal Gaussian feed, with an edge taper of 14.0 dB at  $60^\circ$  for the highest antenna efficiency, along the x-axis and y-axis on the focal plane. From the figure it is clear the high scanning losses inherent in a shape system, but also the lack of symmetry of scanning losses along the x-axis.

With the range of feed horn apertures under consideration, we expected a minimum scanning gain loss of the order of 0.6 dB for the 15.3 cm diameter feeds, and up to 1.5 dB for the 26.0 cm  $TE_{11}$  mode horns for the peripheral pixels around the center. In addition, for array rotations, the pixel-to-pixel variations are of the order of 0.2 dB for the 15.3 cm feed horns and of 0.6 dB for the 26.0 cm horn.

Figure 5.5 shows the Beam deviation vs. feed displacement at the same frequency. From this data we obtained the image scales in the focal plane, which are also asymmetric along the x-axis (see Table 5.1).

**Table 5.1 Image Scales**

Scanning Axis		Image Scale [arcsec/mm]
x	$0 > x$	1.842
x	$0 < x$	1.662
y	$0 <  y $	1.460

This asymmetry will cause the footprint of the array pixels to move in ellipses in the sky when the array is rotated around the center.

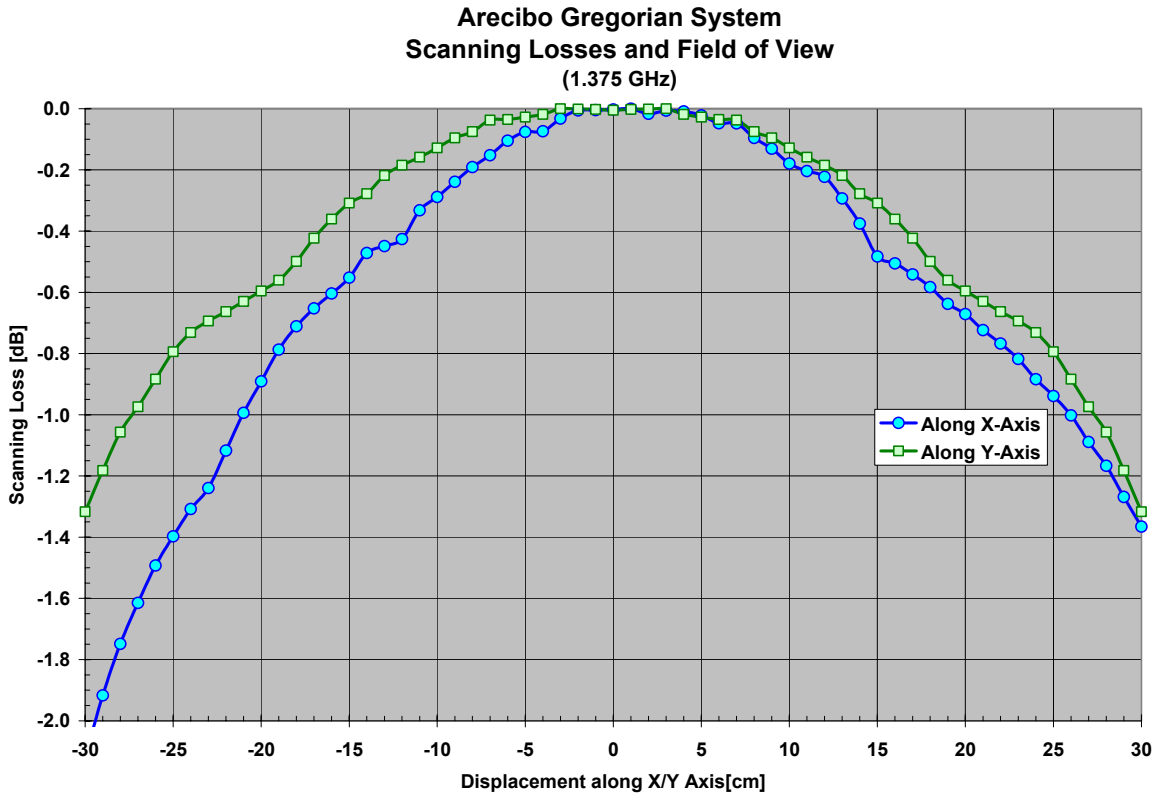


Figure 5.4 Scanning Losses at the Focal Plane of Arecibo Gregorian System (1.375GHz)

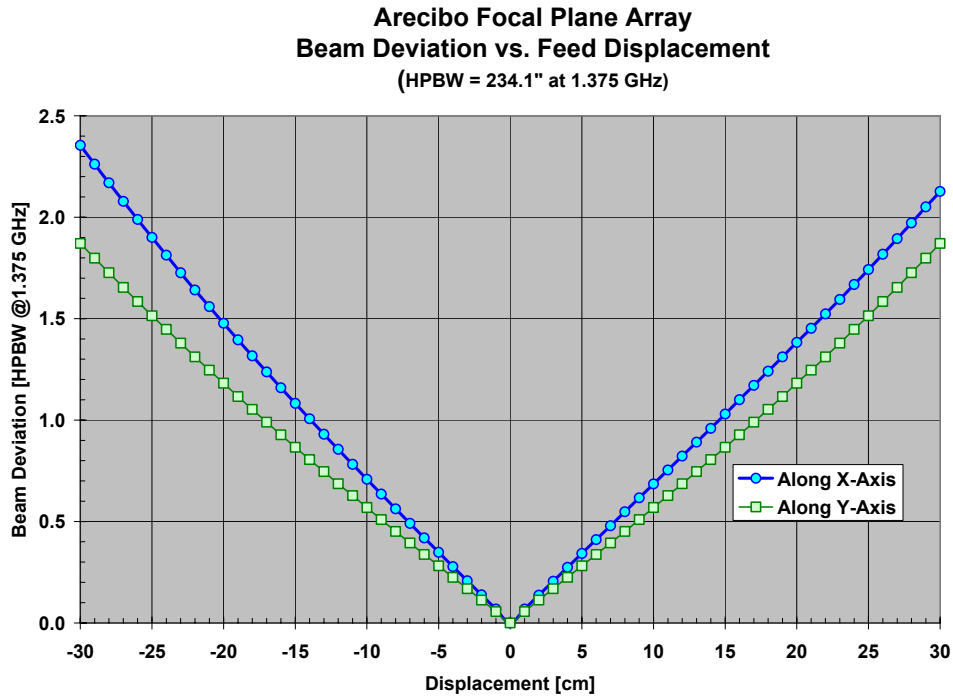
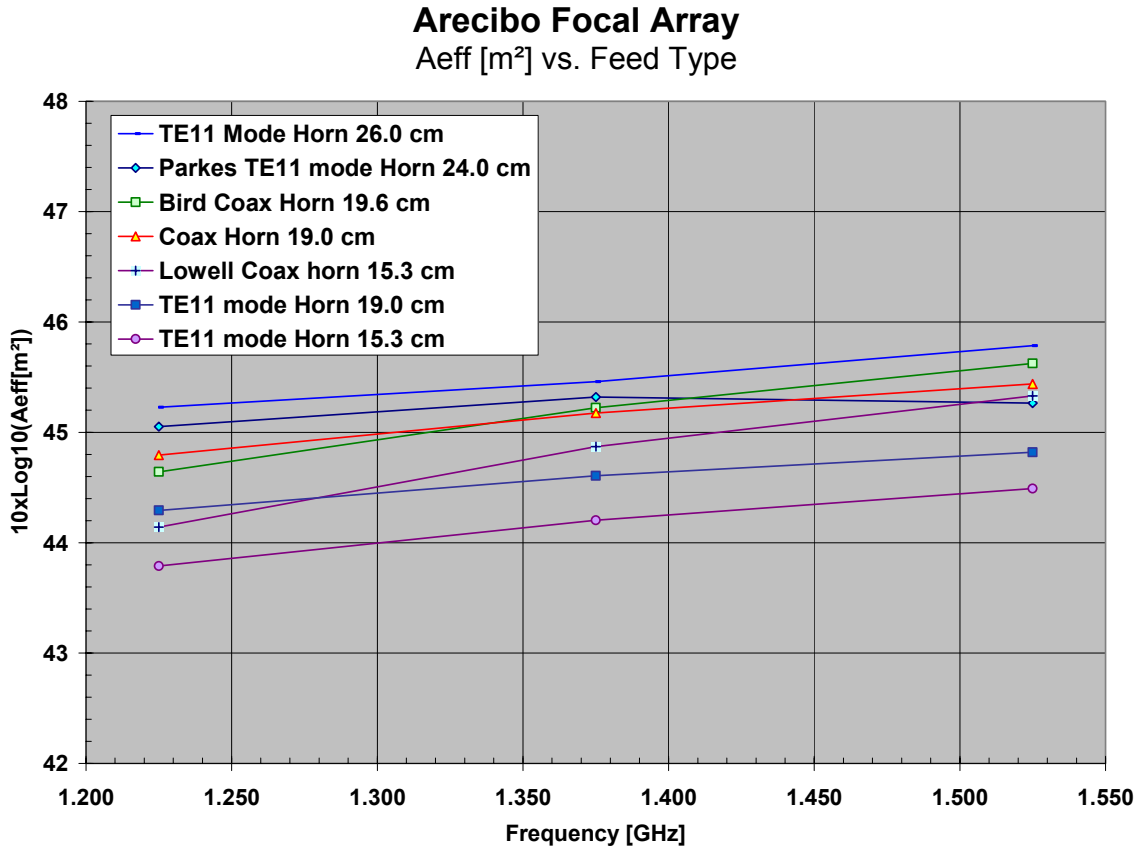


Figure 5.5 Beam deviation vs. Feed displacement (1.375GHz)

## 6. Overall Array Performance

### 6.1 Central Pixel Antenna Effective Aperture/Gain vs. Frequency

We made an initial comparison between the different horn types in terms of the antenna effective aperture shown here in Figure 6.1, in the form:  $10 \times \text{Log}_{10}(\text{Aeff}[\text{m}^2])$ , as a function of frequency.



**Figure 6.1 Antenna Effective Aperture at Pixel # 0 vs. frequency and Feed Type**

From the figure we observe that the 26.0 cm TE<sub>11</sub> mode horn resulted in the highest aperture efficiency/gain, followed by the 24.0 cm diameter Parkes horn, in the lower half of the frequency band, and by the 19.6 coaxial horn in the upper half of the frequency band.

The minimum antenna aperture efficiency/gain is produced by the TE<sub>11</sub> mode horn with 15.3 cm in diameter.

We notice that coaxial horns have intrinsically better gain than TE<sub>11</sub> mode horns with the same aperture diameter.

The iris matching used in the 15.3 and 19.6 coaxial horns produces a steeper frequency response than the TE<sub>11</sub> mode horns of the same diameter. This makes the antenna effective aperture of the array more frequency dependent for coaxial horns than TE<sub>11</sub> mode horns.

A summary of the antenna gain of the central pixel is presented in Table 6.1

**Table 6.1 Summary Antenna Gain, Pixel #0 vs. Horn Type and Frequency**

Frequency [GHz]		1.225	1.375	1.525
Horn Type	Diameter	Gain [dBi]	Gain [dBi]	Gain [dBi]
TE <sub>11</sub> Mode	15.3cm	67.0	68.4	69.6
Coaxial	15.3cm	67.4	69.1	70.5
TE <sub>11</sub> Mode	19.0cm	67.5	68.8	69.9
Coaxial	19.0cm	68.0	69.4	70.6
Bird's Coaxial	19.6 cm	67.9	69.4	70.7
Parkes TE <sub>11</sub> Mode	24.0 cm	68.3	69.5	70.4
TE <sub>11</sub> Mode	26.0 cm	68.4	69.7	70.9

## 6.2 Antenna Effective Aperture for each Pixel vs. Frequency

Next we proceed to analyze the antenna aperture efficiency/gain for each individual array and feed type.

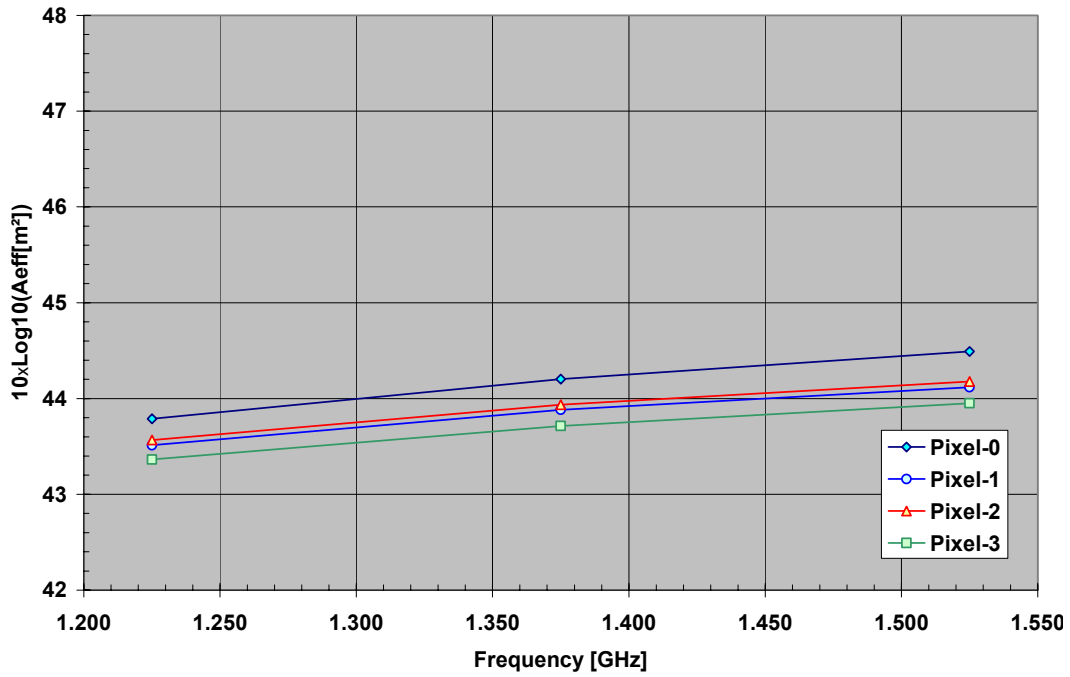
Figure 6.2 presents the effective aperture for an array based on the 15.3 cm set of coaxial and TE<sub>11</sub> mode horn.

Figure 6.3 presents the effective aperture for an array based on the 19.0 cm set of coaxial and TE<sub>11</sub> mode horn.

The effective aperture for an array based on the 19.6 cm coaxial is shown in Figure 6.4, and Figure 6.5 for an array based on the 24.0cm TE<sub>11</sub> mode horn, respectively.

And finally, the effective aperture for an array based of the 26.0cm TE<sub>11</sub> mode horn is shown in Figure 6.6.

**Arecibo Focal Array**  
**A<sub>eff</sub> vs. Frequency**  
**(TE11 Mode Horn: 15.3 cm Diameter)**



**Arecibo Focal Array**  
**A<sub>eff</sub> vs. Frequency**  
**(Lovell's Coaxial Horn: 15.3 cm Diameter)**

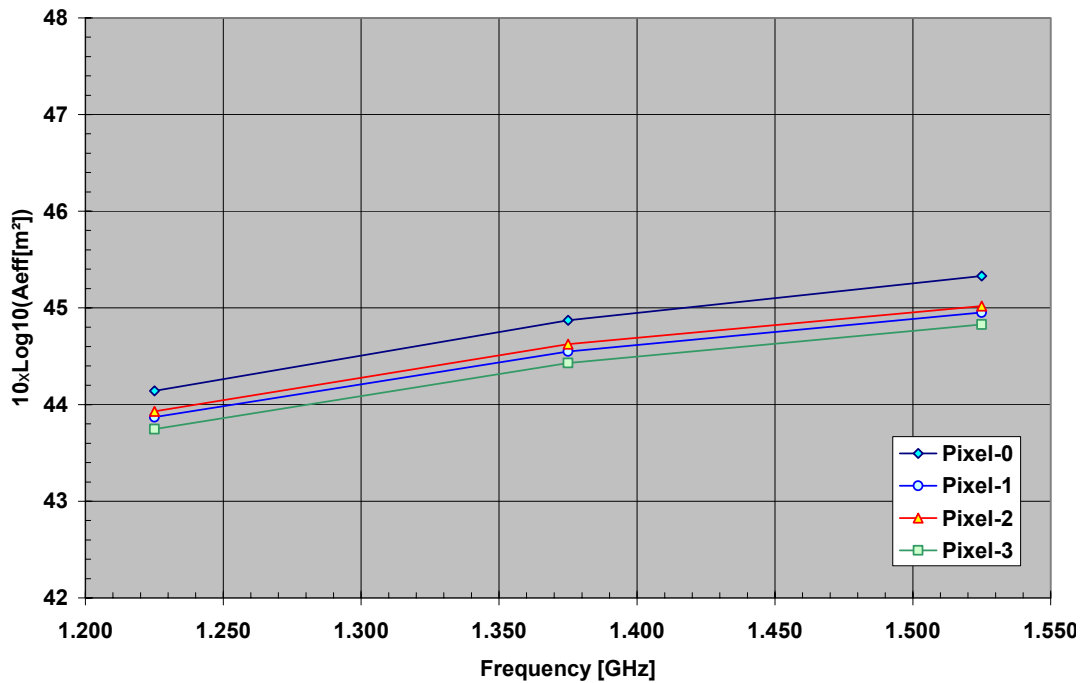
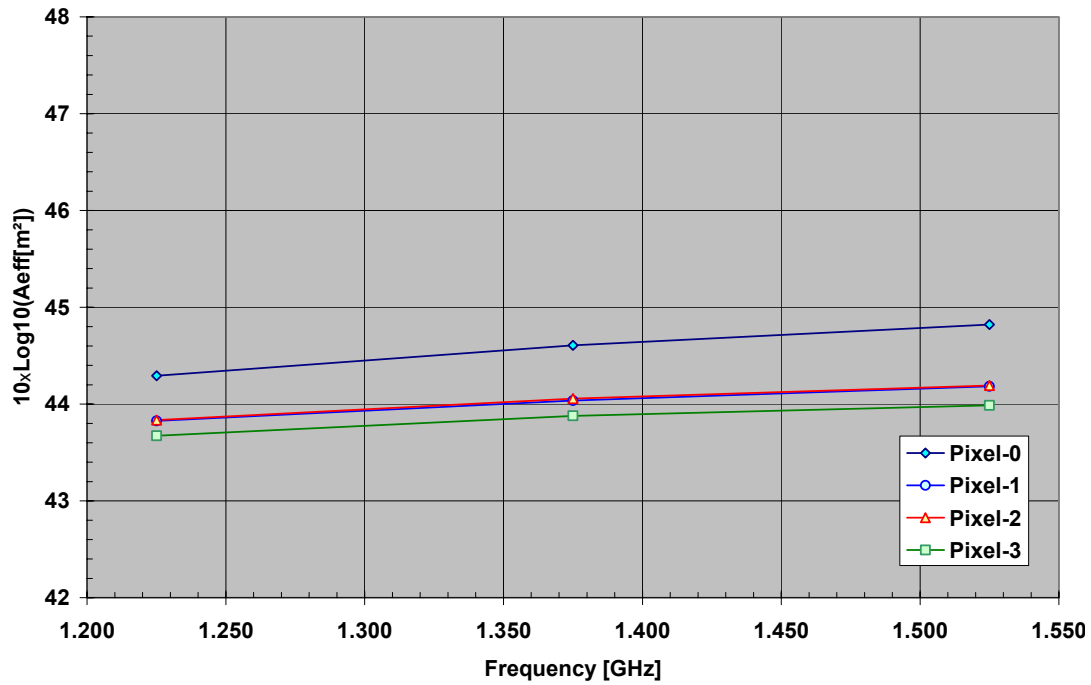


**Figure 6.2 Antenna Effective Aperture for pixel #-0 through pixel #- 3 vs. frequency for horn aperture diameter of 15.3 cm**

**Arecibo Focal Array  
Aeff vs. Frequency  
(TE11 Mode Horn: 19.0 cm Diameter)**



**Arecibo Focal Array  
Aeff vs. Frequency  
(Coaxial Horn: 19.0 cm Diameter)**

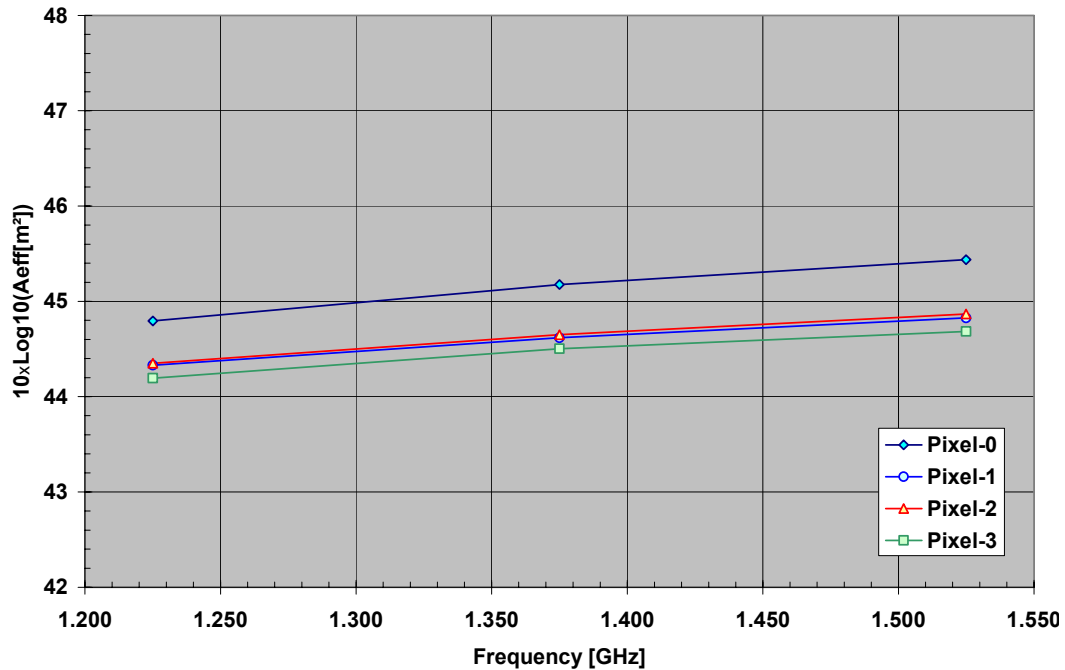


**Figure 6.3 Antenna Effective Aperture for pixel #-0 through pixel #- 3 vs. frequency for horn aperture diameter of 19.0 cm**

**Arecibo Focal Array**  
**A<sub>eff</sub> vs. Frequency**  
**(Bird's Coaxial Horn: 19.6 cm Diameter)**

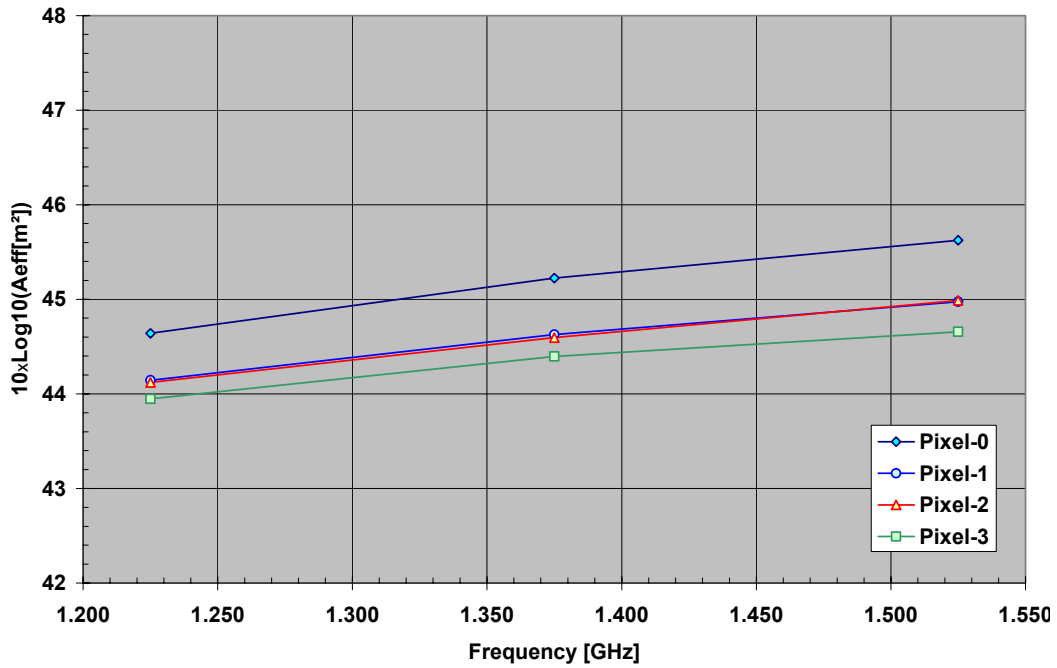


**Figure 6.4 Antenna Effective Aperture for pixel #-0 through pixel #- 3 vs. frequency for Dr. Bird's coaxial horn (19.6 cm)**

**Arecibo Focal Array**  
**A<sub>eff</sub> vs. Frequency**  
**(Parkes TE<sub>11</sub> Mode Horn: 24.0 cm Diameter)**

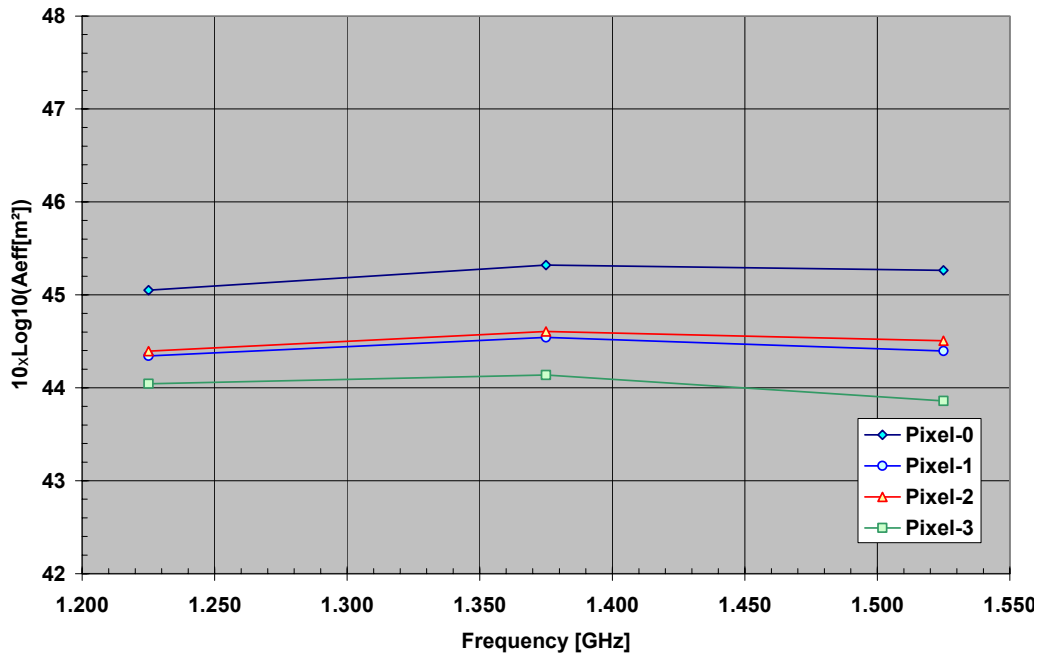


**Figure 6.5 Antenna Effective Aperture for pixel #-0 through pixel #- 3 vs. frequency for Parkes TE<sub>11</sub> mode Horn (24.0cm)**

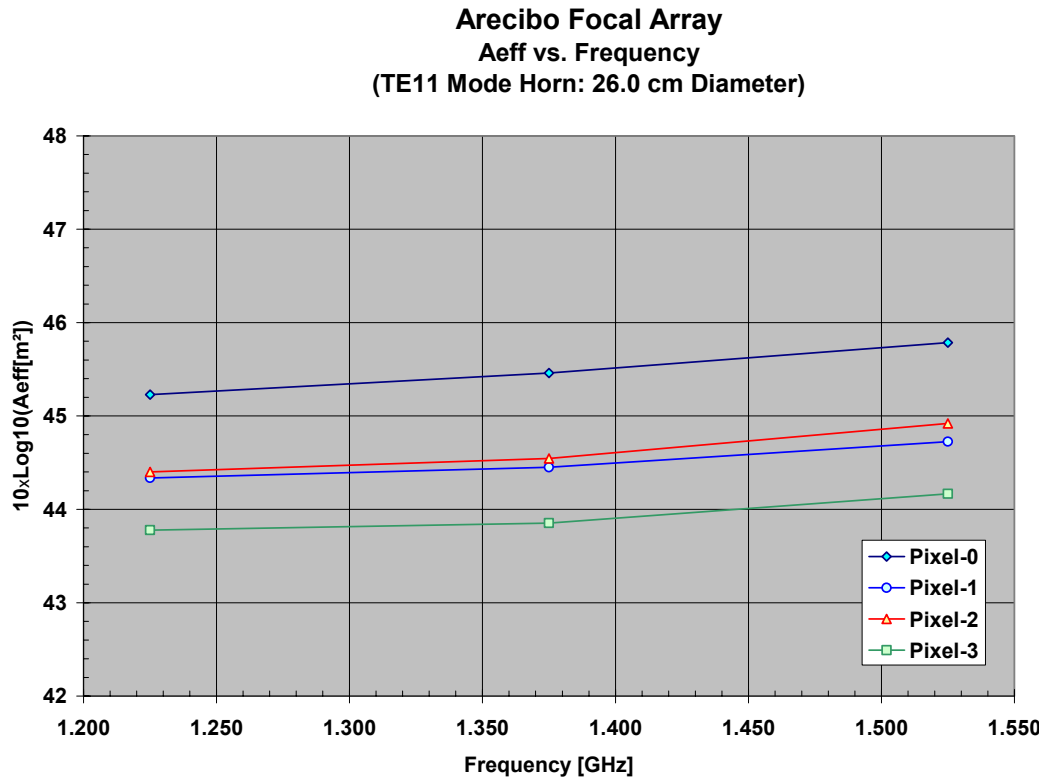


**Figure 6.6 Antenna Aperture Efficiency for pixel #-0 through pixel #- 3 vs. frequency for horn aperture diameter of 26.0 cm**

### 6.3 Discussion

From these results we have the following observations:

- In all cases, the central pixel #0 has the highest antenna aperture efficiency/gain response, as expected.
- The antenna aperture efficiency /gain associated with Pixel #1 and #2 have very similar frequency dependence.
- Pixel #3 has the lowest antenna aperture efficiency/gain vs. frequency response since scanning losses are higher for  $x < 0$  than for  $x > 0$ .
- The larger the aperture diameter of the horn, the larger the gain difference between pixels. On the other hand the larger the horn (i.e., TE<sub>11</sub> mode 26.cm horn) the more efficient is the horn and the higher the system gain.
- The 26.0 cm TE<sub>11</sub> mode horn results in the highest antenna aperture efficiency /gain, with the largest gain difference between pixels, followed by the 24.0 cm diameter Parkes horn.
- The 15.3cm TE<sub>11</sub> mode horn produces the lowest gain.
- Coaxial horns have higher gain than TE<sub>11</sub> mode horns with the same aperture diameter.
- Now, for all pixels, the iris matching used in the 15.3 cm and 19.6 cm coaxial horns produces a steeper frequency response than TE<sub>11</sub> mode horns.
- The antenna gain of all horns surrounding the central pixel is very similar for all coaxial horns and the last two TE<sub>11</sub> mode horns analyzed. Therefore, a Gain/Noise Temperature analysis is required to differentiate further between horn types.

## 7. Feed array and Antenna G/T Performance

For purposes of comparison of the noise performance of all the different feeds inside the optics of the Arecibo Gregorian System, we will assume that the noise contribution of feeds LNA's, and matching, etc, is the same for each feed type, and therefore it is excluded from the noise analysis.

The calculated antenna noise temperature  $T_A$ , will depend on how the particular feed radiation pattern couples with the optics of the Arecibo Gregorian System. Therefore, the noise analysis requires a full  $0 \leq \theta \leq 180$  deg feed pattern.

### 7.1 Antenna Noise Analysis Assumptions

We made the following assumptions in order to obtain the antenna noise temperature at the feed's ports.

- The temperature “seen” by the feed through its radiation pattern mainly determines the antenna noise temperature, measured at the feed's ports.
- To this effect, we assumed that all optical surfaces (main dish, secondary and tertiary reflector) used in the simulation are perfect electric conductors with zero emissivity. All other surfaces are considered perfect black bodies at a given temperature. Any ray terminated in these surfaces is completely absorbed.
- Hence, the temperature seen by the feed in a given direction will depend on the temperature of the last surface reached by the electromagnetic energy pattern after bouncing from one reflector to another.
- We include in this calculation the optical surfaces (main, secondary and tertiary mirrors), the tertiary noise skirt, rotating feed floor, feed room walls and framing, the Gregorian dome and a 1.2 m diameter circular plate centered below the rotating feed floor, for noise control.
- We assumed that the noise temperature of Pixels #1, #2 and #3 is the same as the central pixel #0.
- The Gregorian dome, rotating feed room floor, feed room walls are considered black bodies, with the following temperature map:
  - The noise temperature of the lower portion of the Gregorian dome is assumed to be 180 K instead of 300 K to account for energy that is reflected back to the main dish and to the sky.
  - The noise temperature of the upper portion of the dome (inside) is assumed to be 300 K
  - The noise temperature associated with the rotary feed floor is assumed to be 220K
  - We assumed a noise temperature of 250 K for the framing of the feed room
  - The sky is at 4 K, and the ground at 300 K

Figure 7.1, next, shows a detail of the surfaces associated with the noise temperature calculation.

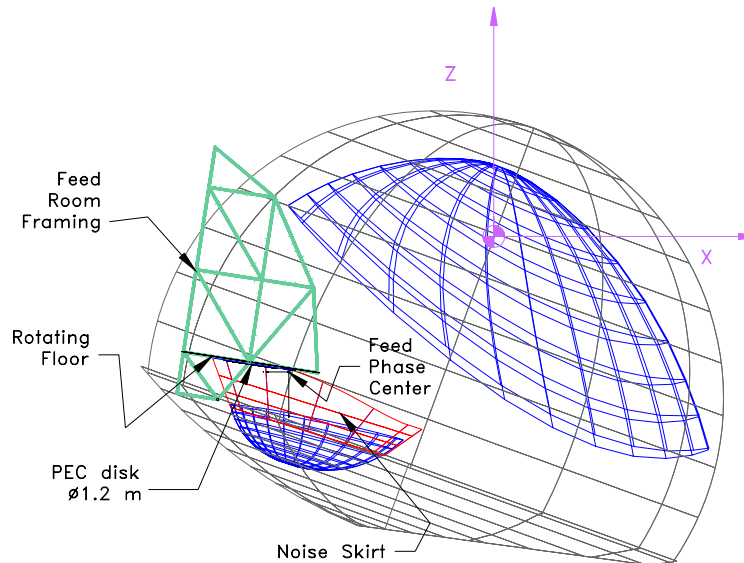


**Table 7.1 Detail of Surfaces used in Noise Temperature Calculation**

## 7.2 Antenna G/T for each Pixel vs. Frequency

Now, in Figures 7.2 through 7.5 we present the calculated G/T and noise temperature of each individual array vs. frequency, for all the feed types.

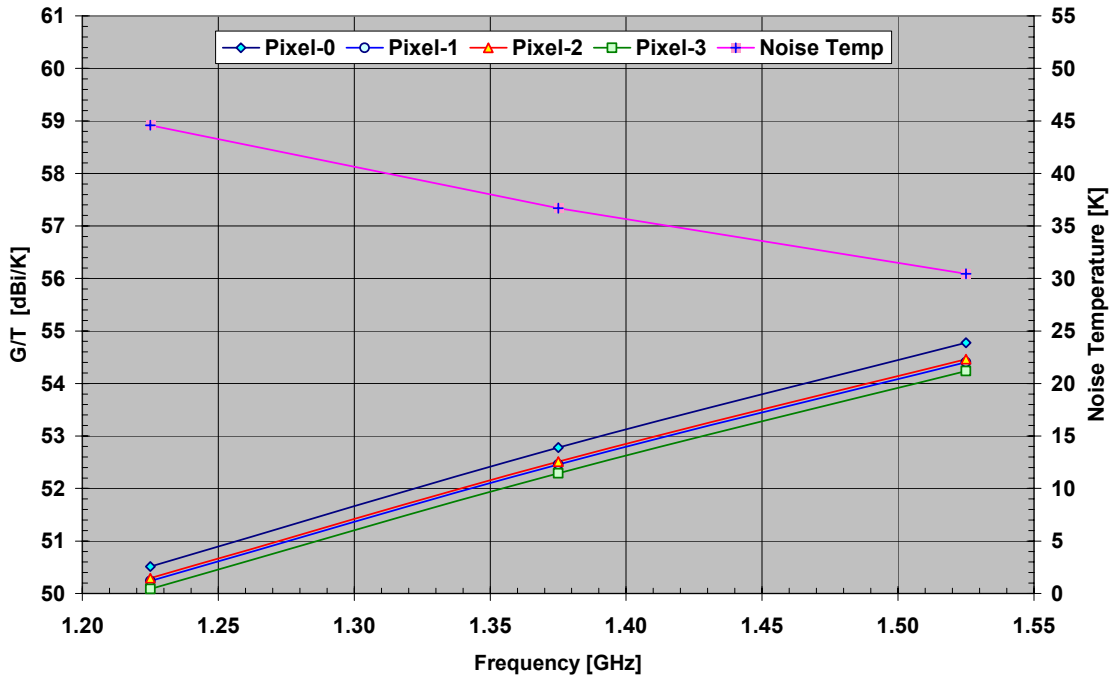
Figure 7.2 corresponds to the G/T of the array based on the 15.3 cm aperture coaxial and  $TE_{11}$  mode horn set.

Figure 7.3 presents the calculated G/T corresponding to array based on the 19.0 cm aperture coaxial and  $TE_{11}$  mode horn set.

Figure 7.4 shows the G/T of Dr. Bird's 19.6 cm coaxial horn array and Parkes 24.0 cm  $TE_{11}$  mode horn array.

Figure 7.5 shows the G/T and noise temperature of the array based on the 26.0 cm  $TE_{11}$  mode horn.

**Arecibo Focal Array**  
**G/T vs. Pixel**  
**(TE11 Mode Horn: 15.3 cm Diameter)**



**Arecibo Focal Array**  
**G/T vs. Pixel**  
**(Lovell's Coaxial Horn 15.3 cm Diameter Opt)**

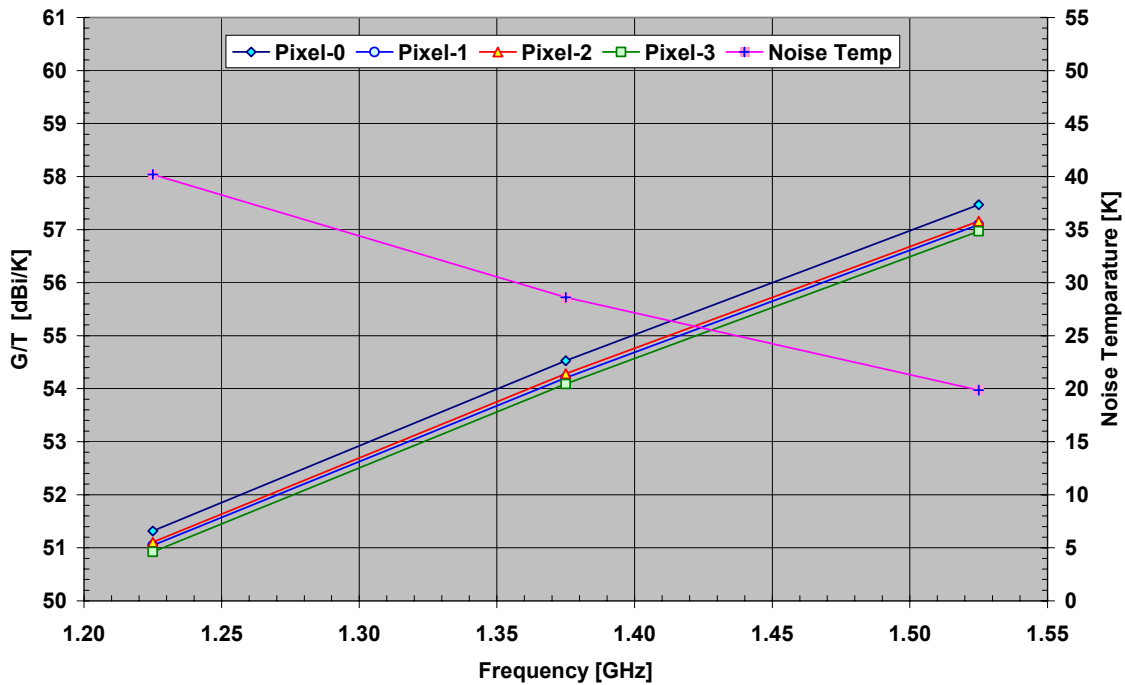
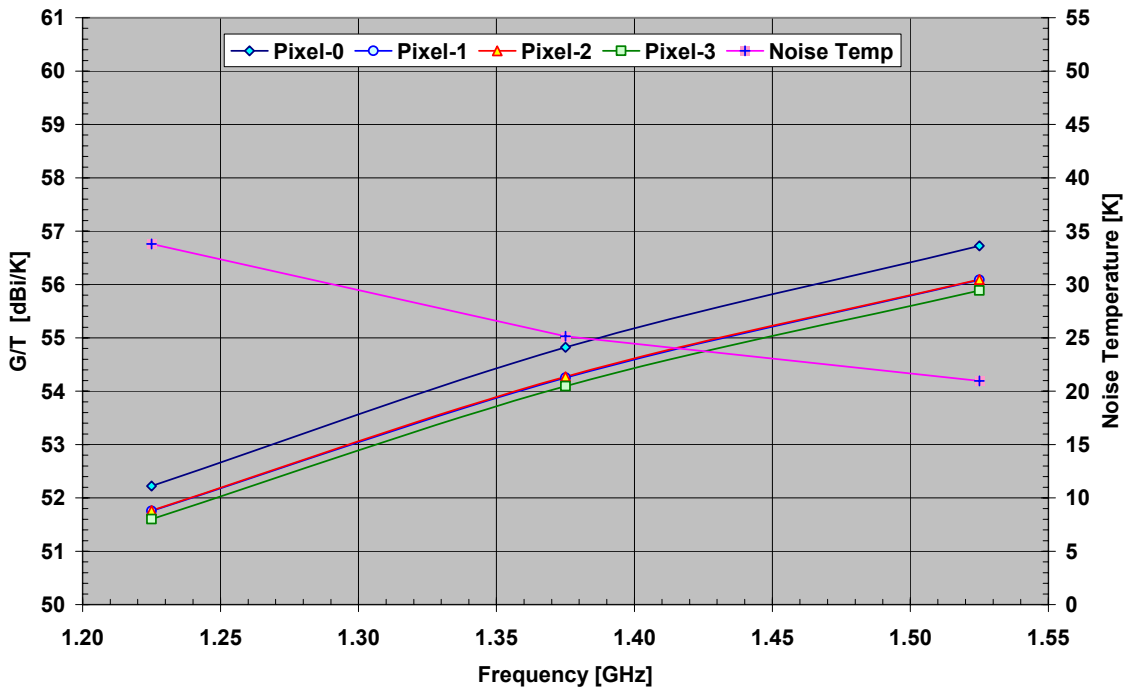
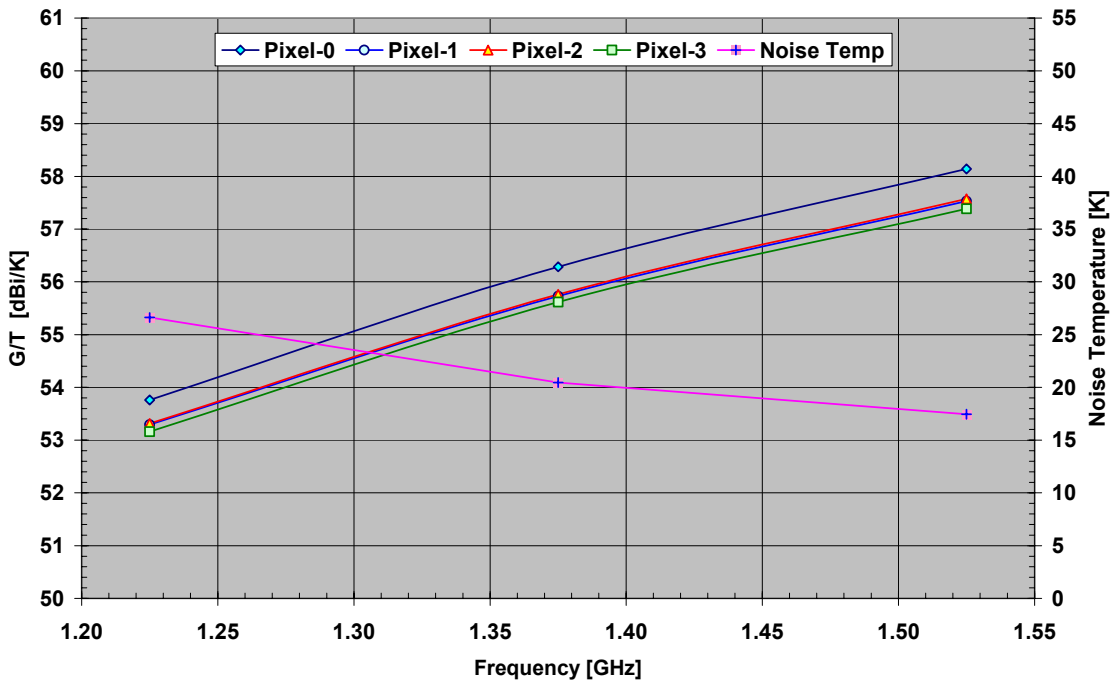


Figure 7.2 Antenna  $G/T_A$  [dBi/K] for pixel #-0 to pixel #- 3 vs. frequency (diam 15.3 cm)

**Arecibo Focal Array**  
**G/T vs. Pixel**  
**(TE11 Mode Horn: 19.0 cm Diameter)**

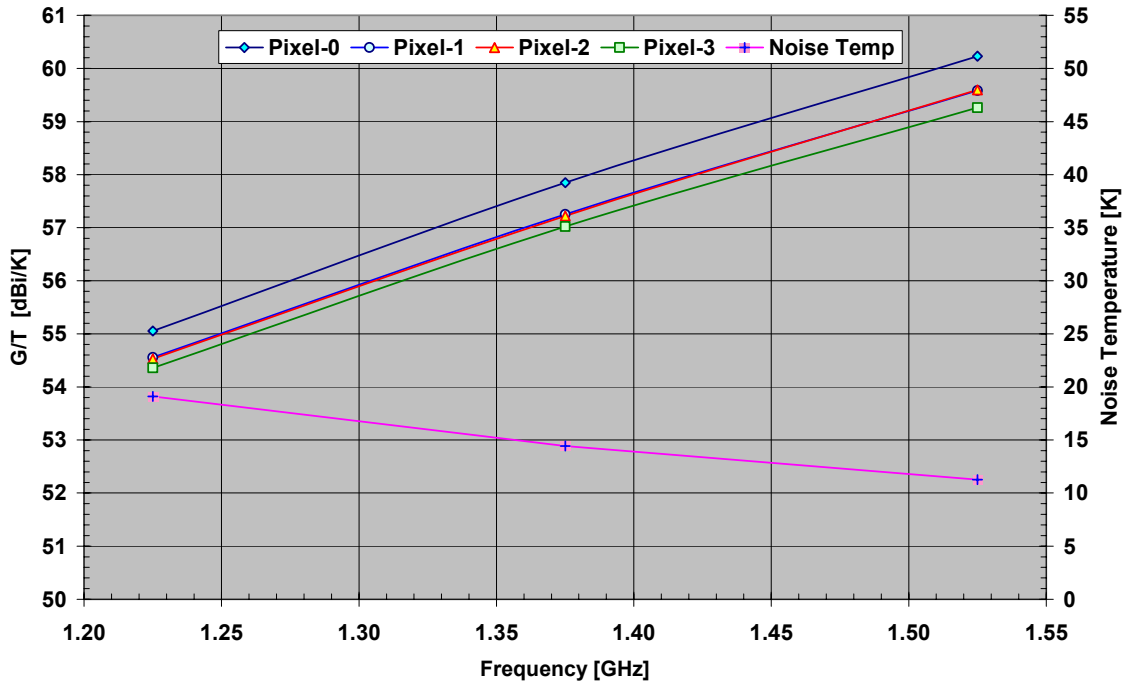


**Arecibo Focal Array**  
**G/T vs. Pixel**  
**(Coax Horn: 19.0 cm Diameter)**



**Figure 7.3 Antenna  $G/T_A$  [dBi/K] for pixel #-0 through pixel #- 3 vs. frequency for horn aperture diameter of 19.0 cm**

**Arecibo Focal Array**  
**G/T vs. Pixel**  
**(Coax Horn: 19.6 cm Diameter)**



**Arecibo Focal Array**  
**G/T vs. Pixel**  
**(Parkes TE<sub>11</sub> Horn: 24.0 cm)**

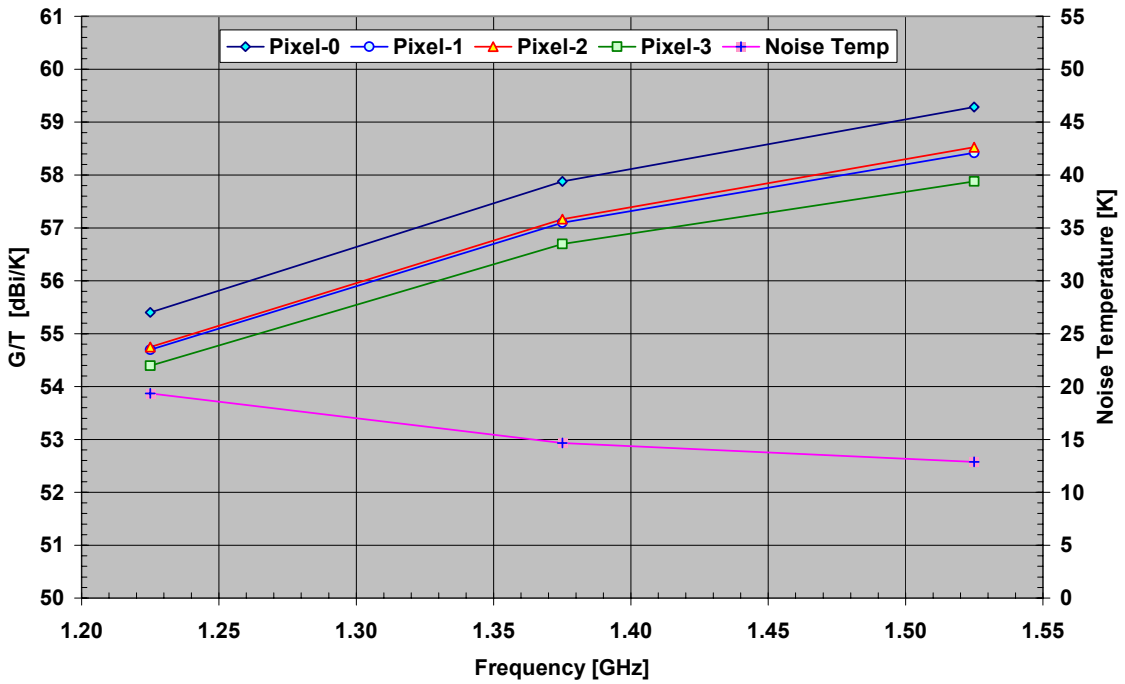


**Figure 7.4 Antenna G/T<sub>A</sub> [dBi/K] for pixel #-0 through pixel #- 3 vs. frequency for Bird's coaxial horn (19.0 cm) and Parkes TE<sub>11</sub> Horn (24.0cm)**

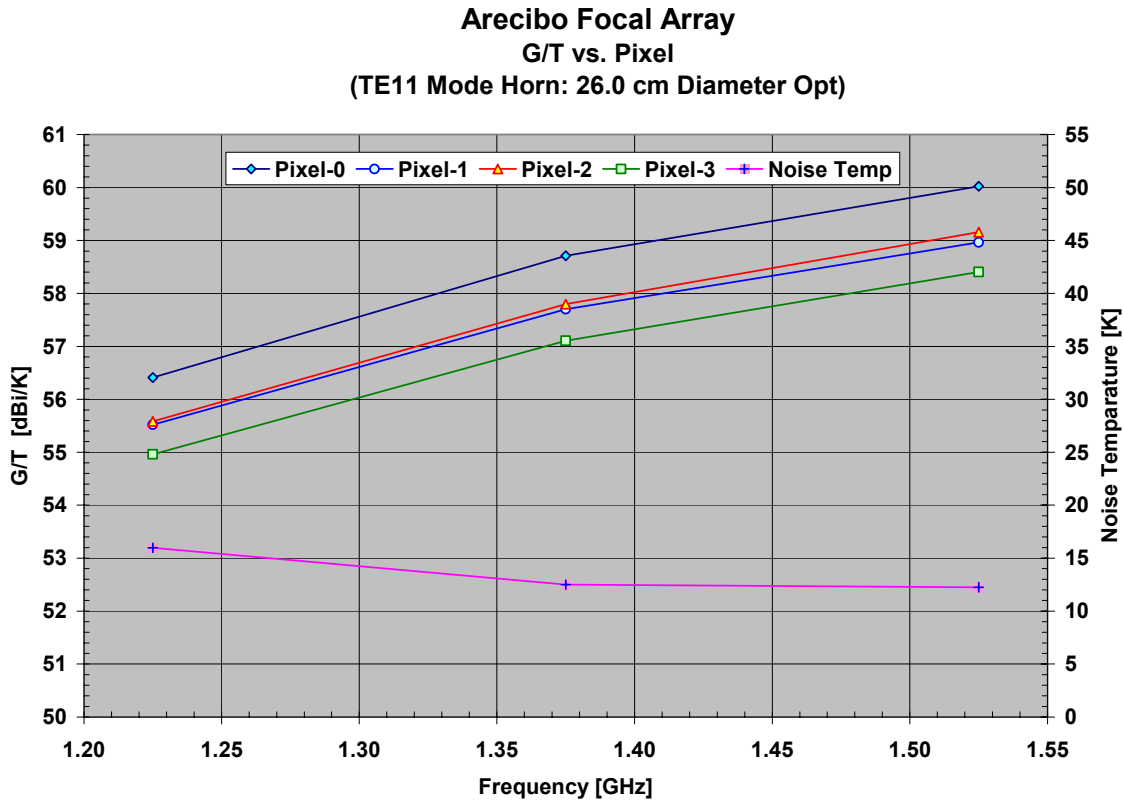


Figure 7.5 Antenna  $G/T_A$  [dBi/K] for pixel #-0 through pixel #- 3 vs. frequency for horn aperture diameter of 26.0 cm

### 7.3 Discussion

The inclusion of the noise temperature contribution of the feed radiation pattern in the horn performance analysis helps to make a distinction between horns:

- Coaxial horns have higher  $G/T$  performance than  $TE_{11}$  mode horns with the same aperture diameter.
- The 60 cm back plate used in Dr. Bird’s 19.6 cm coaxial horn improves greatly the  $G/T$  ratio by reducing the back lobe radiation.
- Again, coaxial horns have steeper  $G/T$  frequency dependence than  $TE_{11}$  mode horns with the same aperture diameter.
- We notice a reduction in noise contribution with the increasing horn aperture.
- We notice that Parkes 24.0 cm  $TE_{11}$  mode horn and 26.0 cm  $TE_{11}$  mode horn have better  $G/T$  over the low and medium frequency range than Dr. Bird’s 19.6 cm coaxial horn.
- Dr. Bird’s 19.6 cm coaxial horn has the best  $G/T$  at 1.525 GHz.

## 8. Summary and Conclusions

Figures 8.1 and 8.2 summarize the antenna performance in terms of Antenna gain and Effective Aperture/T of the array for all pixels and all the feeds considered in this study. The abscise feed type number is the same that appears in Table 1.1. Notice also that there are three frequency points associated with each pixel and feed type.

### 8.1 Conclusions

- We have analyzed seven horns ( $TE_{11}$  mode and coaxial) with different aperture diameters in terms of radiation patterns, antenna gain, antenna G/T for the Arecibo Multibeam System.
- By studying horns of increasing aperture diameters we have found that the array's optimum illumination is obtained with a horn aperture of 26.0 cm ( $TE_{11}$  mode in this study). The array performance of larger horn diameters is dominated by scanning losses.
- We have found that coaxial horns have better G/T performance compared with  $TE_{11}$  mode horn with the same aperture diameter.
- Irises matched coaxial horns tend to have steeper G/T frequency slope than  $TE_{11}$  mode horns.
- We have found that Dr. Bird's 19.6 cm coaxial horn has the best marginal G/T performance at 1.525 GHz. It could be conceivable to use a back lobe reduction scheme for the full array, similar to the 60 cm diameter back plate used in this particular horn.
- From the set of feed horns analyzed, the 26.0 cm diameter,  $TE_{11}$  mode horn yields the best G/T overall performance over the frequency band.
- The 15.3cm  $TE_{11}$  mode horn has the lowest G/T.

Pixel-to-Pixel Gain variations:

- The central pixel in all cases has a better Gain and better G/T when compared with the other pixels in the array.
- Pixel #1 and Pixel #2 have similar frequency response.
- Pixel #3 has the lower frequency response, since the scanning losses are higher for  $x < 0$  than for  $x > 0$ .
- The maximum difference in G/T between pixels varies from a minimum of 0.5 dB/T, for Lovell's 15.3 cm coaxial horn array, to a maximum of 1.6 dB/K in the case of the 26.0 cm  $TE_{11}$  mode array, in both cases between pixel #0 and pixel #3 at 1.525 GHz.

### Arecibo Gregorian Array Antenna Gain

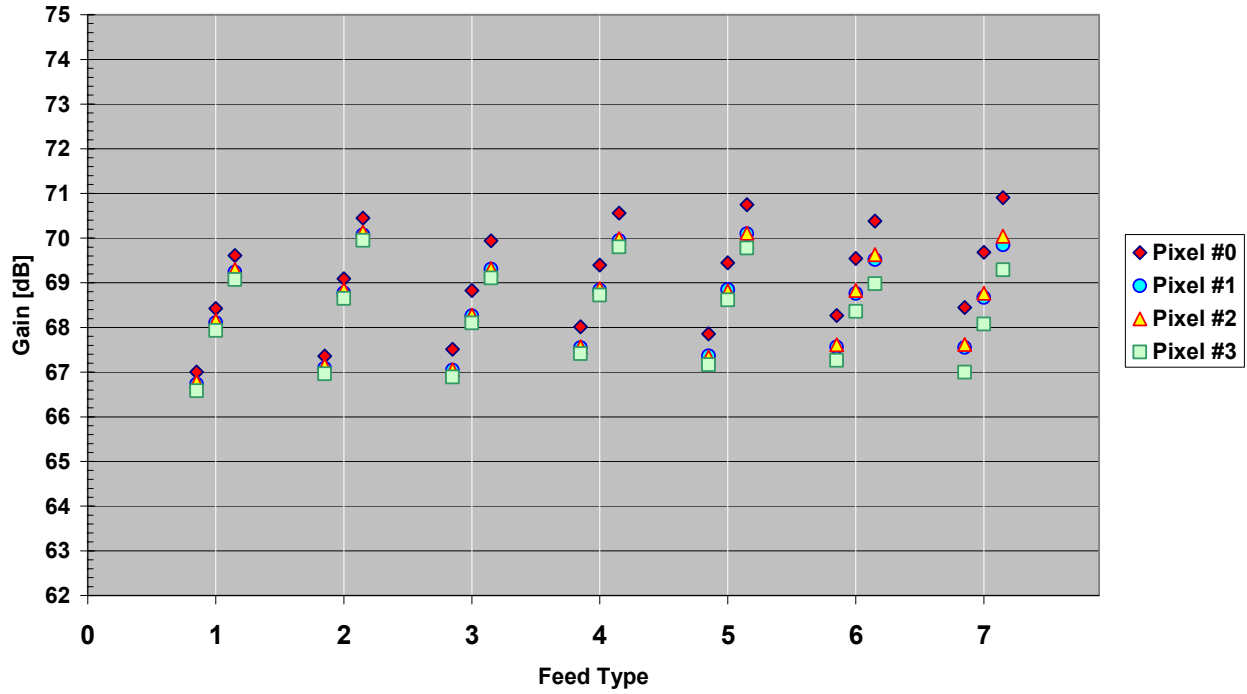


Figure 8.1 Antenna Gain for all pixels and frequencies vs. feed types

### Arecibo Gregorian Array Aeff/T Performance

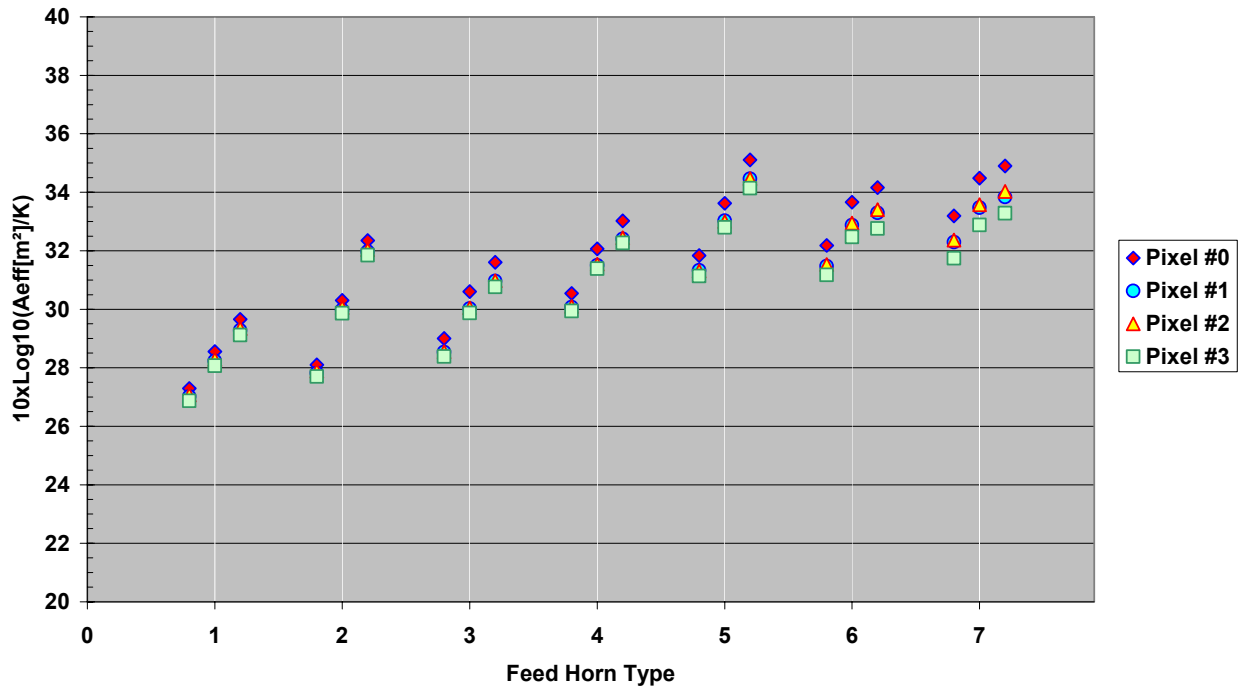


Figure 8.2 Antenna Aeff/T for all pixels and frequencies vs. feed types

- Pixel-to-Pixel variations may be reduced by,
  1. Displacing the whole array a few cm in the direction  $x > 0$ . This approach will increase the gain of pixel #3 at the expense of higher scanning losses for the other pixels. Nevertheless, the gain of the central pixel will be still higher than the others; therefore, we need to combine this solution with the following one.
  2. Reducing the aperture of the central pixel. If the walls of surrounding pixels are not touching each other, this will allow to move them closer, decreasing in turn its scanning losses. The required diameter, for the case of a horn like Parkes, will be approximately 22.0 cm to match the central pixel gain with the others. This solution will require the design of two feeds instead of one.
- Finally it is the issue of sky footprint. For the Parkes horn at 1.375 GHz, the minimum beam deviation in the sky is 1.45 HPBW, (about 5.66'). Since image scale is slightly asymmetric, the array's footprint in the sky will move in ellipses as we rotate the array, with a maximum variation of 0.36 HPBW for a 24.0 cm diameter horn. Therefore, the maximum acceptable beam separation in the sky sets an additional constraint to the maximum horn diameter for the array.